BIOCHEMISTRY

Perturbation of NAD(P)H metabolism with the *Lb*NOX xenotopic tool extends lifespan and mitigates age-related changes

Shweta Yadav[1]†, Xingxiu Pan[2]†, Shengxi Li[3], Paige LaRae Martin[1], Ngoc Hoang[1], Kejin Chen[1], Aditi Karhadkar[1], Jatin Malhotra[1], Austin L. Zuckerman[2,4], Subrata Munan[2], Markus K. Klose[5], Lin Wang[3], Valentin Cracan[2,6]*†, Andrey A. Parkhitko[1,7]*†

Aging involves widespread metabolic dysregulation, including a decline in total nicotinamide adenine dinucleotide (NAD) levels. While NAD precursor supplementation elevates total NAD levels, it does not reveal tissue-specific effects of an altered NADH [reduced form of NAD^+ (oxidized NAD)]/NAD^+ balance. To address this, we generated transgenic *Drosophila* expressing the genetically encoded xenotopic enzyme *Lb*NOX, which converts NADH to NAD^+. *Lb*NOX expression modulated both NAD(H) and NADP(H) (reduced form of NAD phosphate) metabolites in a sex-dependent manner and rescued neuronal cell death induced by mutant αB-crystallin–associated reductive stress. We demonstrate that tissue-specific targeting of redox NAD metabolism shows distinct outcomes: Muscle-specific *Lb*NOX expression confers stronger protection against paraquat-induced oxidative stress than whole-body expression, emphasizing tissue-dependent redox sensitivity. Notably, *Lb*NOX expression in nonneuronal tissues restored youthful sleep patterns in aged flies. Together, these findings establish *Lb*NOX as an efficient xenotopic tool for in vivo redox manipulation and reveal tissue- and sex-specific NAD(P)H mechanisms underlying aging, stress resilience, and sleep regulation, providing a framework for NAD-based interventions in aging.

INTRODUCTION

Metabolic dysregulation represents one of the major driving forces in aging, leading to impaired organismal fitness, an age-dependent increase in susceptibility to diseases, a decreased ability to mount a stress response, and increased frailty (*1*). Dysregulation of nicotinamide adenine dinucleotide (NAD) metabolism has emerged as a contributing factor in the pathogenesis of aging and multiple age-related diseases (*2*–*4*). NAD in cells is found in both oxidized (NAD^+) and reduced (NADH) forms, which together furnish cells with a key NADH/NAD^+ redox pair that sits at the core of redox metabolism and signaling (*5*). In addition, NAD^+ also serves as an essential substrate for nonredox NAD^+-dependent enzymes, including sirtuins, CD38, ARTs, SARM1, and poly(ADP-ribose) polymerases (*5*, *6*).

The total NAD pool declines with age and under various pathological conditions in a tissue-specific manner, potentially contributing to the exacerbation of the pathological state. However, whether this occurs universally across different species and tissues remains unclear (*7*). Multiple preclinical studies in rodents provide evidence of the beneficial effects of supplementation with NAD biosynthetic precursors that boost total cellular NAD levels (*7*–*10*). However, supplementation studies do not provide an assessment of the tissue-specific role of restoring NAD levels or how does the NADH/NAD^+ redox potential itself regulates the aging process.

Here, we used an alternative approach to directly manipulate NADH/NAD^+ ratio by introducing an enzyme from a different species ("xenotopic approach") (*11*). We used *Lactobacillus brevis* H_2O-forming NADH oxidase (*Lb*NOX) (*12*) as a genetically encoded xenotopic tool previously used for a compartment-specific decrease of the NADH/NAD^+ ratio in living cells. We reasoned that a prooxidative shift (a decrease) in NADH/NAD^+ ratio would be beneficial as an elevated NADH/NAD^+ ratio (sometimes referred to as NADH-reductive stress) is linked to various pathological states ranging from primary mitochondrial diseases to neurodegeneration, as well as to aging-associated metabolic changes (*13*–*15*). There are existing genetic tools to express transgenes in *Drosophila*, which allow for targeted expression of *Lb*NOX in different tissues or population of cells. The application of this model system can directly address how manipulation of cellular NADH/NAD^+ ratio affects various organismal processes.

We show that cytosolic *Lb*NOX expression in transgenic *Drosophila* flies affects both NADH/NAD^+ and NADPH [reduced form of NAD phosphate ($NADP^+$)]/$NADP^+$ ratios to a different extent and in a sex-dependent manner. We further show that *Lb*NOX expression promotes resistance to oxidative and starvation stress and extends lifespan and that targeting NAD metabolism in different tissues may have drastically diverse outcomes. Last, we demonstrate that tissue-specific *Lb*NOX expression improves sleep profiles in aged flies back to a youthful state.

In summary, we demonstrate the broad impacts of modulating NADH-consuming activity using the xenotopic tool *Lb*NOX in the context of multiple aging-associated metabolic changes. We anticipate that our work will further clarify tissue-specific roles of NAD metabolism in the aging process and aid in the design of "combinatorial" clinical trials that can target both redox-neutral and redox-dependent

[1]Aging Institute of UPMC, University of Pittsburgh, Pittsburgh, PA, USA. [2]Laboratory of Redox Biology and Metabolism, Scintillon Institute, San Diego, CA, USA. [3]State Key Laboratory of Common Mechanism Research for Major Disease, Institute of Basic Medical Sciences, Chinese Academy of Medical Sciences and Peking Union Medical College, Beijing, China. [4]Program in Mathematics and Science Education, University of California, San Diego and San Diego State University, San Diego, CA, USA. [5]Department of Pharmacology and Chemical Biology, University of Pittsburgh, Pittsburgh, PA, USA. [6]Department of Molecular and Cellular Biology, Scripps Research Institute, La Jolla, CA, USA. [7]Division of Endocrinology and Metabolism, Department of Medicine, University of Pittsburgh, Pittsburgh, PA, USA.
*Corresponding author. Email: vcracan@scripps.edu (V.C.); aparkhitko@pitt.edu (A.A.P.)
†These authors contributed equally to this work.

aspects of NAD metabolism or combine NAD precursors with xenotopic tools.

RESULTS

*Lb*NOX expression alters NAD(P)H/NAD(P)$^+$ ratios in *Drosophila* in a sex-dependent manner

NAD boosters/precursors supplementation can increase organismal NAD levels; however, supplementation studies do not allow for testing tissue-specific roles of an altered NADH/NAD$^+$ ratio in regulating different biological processes, nor can they distinguish the impact of redox reactions from nonredox pathways (*10*). Therefore, we turned our attention to *Lb*NOX as a genetically encoded xenotopic tool for inducing a compartment-specific decrease in the NADH/NAD$^+$ ratio (*12*). *Lb*NOX catalyzes the conversion of NADH to NAD$^+$ generating water as a byproduct (Fig. 1A) (*12*). We cloned *Lb*NOX into the pWALIUM10-roe *Drosophila* expression vector and created transgenic flies carrying the *Lb*NOX transgene on the 2nd (line #128) or on the 3rd (line #129) chromosome at a defined genetic locus. To confirm the expression of *Lb*NOX in flies, we expressed *Lb*NOX in adults ubiquitously using the *tubulin-Gal4, tubulin-Gal80^{ts}* temperature-inducible system (*16*). Gal80^{ts} is active at 18°C and represses Gal4; while at 29°C, Gal80^{ts} is inactivated, allowing for the Gal4-dependent expression of *Lb*NOX. Genetic crosses were set at 18°C and maintained until the progeny eclosed followed by switching to 29°C to induce expression of *Lb*NOX for 7 days. As a control, we used the same parental line that we had injected with the UAS-*Lb*NOX construct to produce the transgenic UAS-*Lb*NOX flies. We confirmed expression of *Lb*NOX in flies by Western blotting (fig. S1A). Although NAD metabolites are known to be compartmentalized within the cell, we decided not to use mitochondria-targeted *Lb*NOX as it will likely dissipate more reduced NADH/NAD$^+$ redox potential (compared to the cytosol) and divert electrons away from oxidative phosphorylation and adenosine 5′-triphosphate production. As we were interested in assessing the effects of altering NADH/NAD$^+$ ratio in aged flies and wanted to explore sex-specific differences, we confirmed that the expression level of *Lb*NOX is similar across male and female flies and at different ages (fig. S1A).

We tested the impact of ubiquitous *Lb*NOX expression on NAD$^+$ levels and related metabolites, i.e., NADH, NADP$^+$, and NADPH in whole flies. Unexpectedly, we observed notably different effects on NAD(P)(H) levels and corresponding redox ratios between male and female flies, which reflects sex-specific alterations (Fig. 1, B to E). In male flies of both transgenic lines 128 and 129, we observed a decrease in NADH, which also translated to a robust decrease in NADH/NAD$^+$ ratio but with no observed effect on the total NAD pool (NAD$^+$ + NADH) (Fig. 1B). At the same time, in female flies of both transgenic lines 128 and 129, neither NADH levels nor the NADH/NAD$^+$ ratio was affected compared to controls, and no alteration in the total NAD pool was observed (Fig. 1C).

*Lb*NOX expression in both male and female flies of the transgenic lines 128 and 129 led to a robust increase in NADPH levels (Fig. 1, D and E) with an increase in NADPH/NADP$^+$ ratio only in the female flies of the line 128 (Fig. 1E). We also observed that the total NADP pool (NADP$^+$ + NADPH) was increased in both females and males in transgenic lines 128 and 129 (Fig. 1, D and E). As an illustration, we plotted on the same graph all four coenzymes NAD$^+$, NADH, NADP$^+$, and NADPH measured in control male and female flies to highlight that the NAD pool is ~20 times larger than the NADP pool and that the NADP pool is mostly in the reduced form (fig. S1, B and C). While total cellular levels of NADH and NADPH are comparable in females, males exhibit a relative enrichment of NADPH over NADH, suggesting potential sex-specific differences in redox homeostasis (fig. S1, B and C). We note that observed impact of *Lb*NOX on both NAD(H) and NADP(H) coenzymes can be due to productive rebalancing between NAD and NADP pools. Recent studies suggest that accumulation of NADH due to dysfunctional electron transport chain (ETC) can affect NADPH production (*17*, *18*). We therefore reasoned that modulation of NADH consumption by *Lb*NOX might explain improved NADPH production in a subset of our experiments.

We intentionally used the TARGET system (*tubulin-Gal4* and *tubulin-Gal80ts*) for biochemical validations as the GeneSwitch (GS) system (used later for lifespan studies) may be leaky, has a weaker expression, and may be mosaic across different cell types, that would mask potential biochemical effects (*19*). In summary, we have created a previously unknown transgenic xenotopic tool that perturbs NAD(P)(H) metabolites in *Drosophila* in a sex-dependent manner.

*Lb*NOX expression rescues neurodegeneration associated with CryAB-induced reductive stress in female flies

Reductive stress is defined as an excessive level of reducing equivalents in the form of NADH, NADPH, or GSH (reduced form of glutathione) (*13*, *15*, *20*) or low abundance of reactive oxygen species (ROS) due to inactive ETC or hyperactivity of the antioxidant systems (*21*). Previous studies have described a model of reductive stress in *Drosophila* via expression of the dominant R120G mutation in the αB-crystallin (CryAB) gene (*CryAB^{R120G}*) (*22*). In humans, the autosomal dominant R120G mutation in the CryAB gene (*CryAB^{R120G}*) manifests as adult-onset cataracts, skeletal muscle weakness, and heart failure (*23*). When mutant CryAB is expressed in *Drosophila* eye, it causes neuronal cell death that can be easily visualized by the appearance of fused glossy disorganized ommatidia under the light microscope (*22*). The current model of *CryAB^{R120G}* reductive stress predicts that overabundance of both NADPH and GSH exacerbates the phenotype where lowering cellular NADPH or GSH levels can ameliorate the observed phenotypes seen in flies expressing *CryAB^{R120G}* (*22*). We decided to explore how sex-dependent modulation of NAD(P)(H) levels imposed by *Lb*NOX expression affects the *CryAB^{R120G}* phenotype in *Drosophila*. *Lb*NOX expression alone did not affect eye morphology in female (Fig. 2A) or male flies (Fig. 2C). As was previously demonstrated, expression of mutant *CryAB^{R120G}* resulted in a strong neuronal cell death phenotype in both female (Fig. 2B) and male flies (Fig. 2D) characterized by loss of pigmentation, presence of fused ommatidia, and extra interommatidial bristles. The phenotype in male flies is relatively drastic with an additional effect of reduced eye size and pronounced loss of pigmentation. Expression of *Lb*NOX transgenic line 128 (but not line 129) completely rescued the neuronal cell death phenotype in female flies (Fig. 2, B and E), while the neuronal cell death phenotype in males was not modified (Fig. 2, D and F). We note that *Lb*NOX expression boosted NADPH levels in both female lines 128 and 129, while it reliably increased NADPH/NADP$^+$ ratio only in line 128, where *Lb*NOX expression completely rescued the *CryAB^{R120G}* phenotype. We also note that the *CryAB^{R120G}* eye phenotype is much more severe in males compared to females (Fig. 2, B and D). The observed rescue with only one line would also rule out the possibility of rescue due to simple Gal4 dilution. *Lb*NOX expression

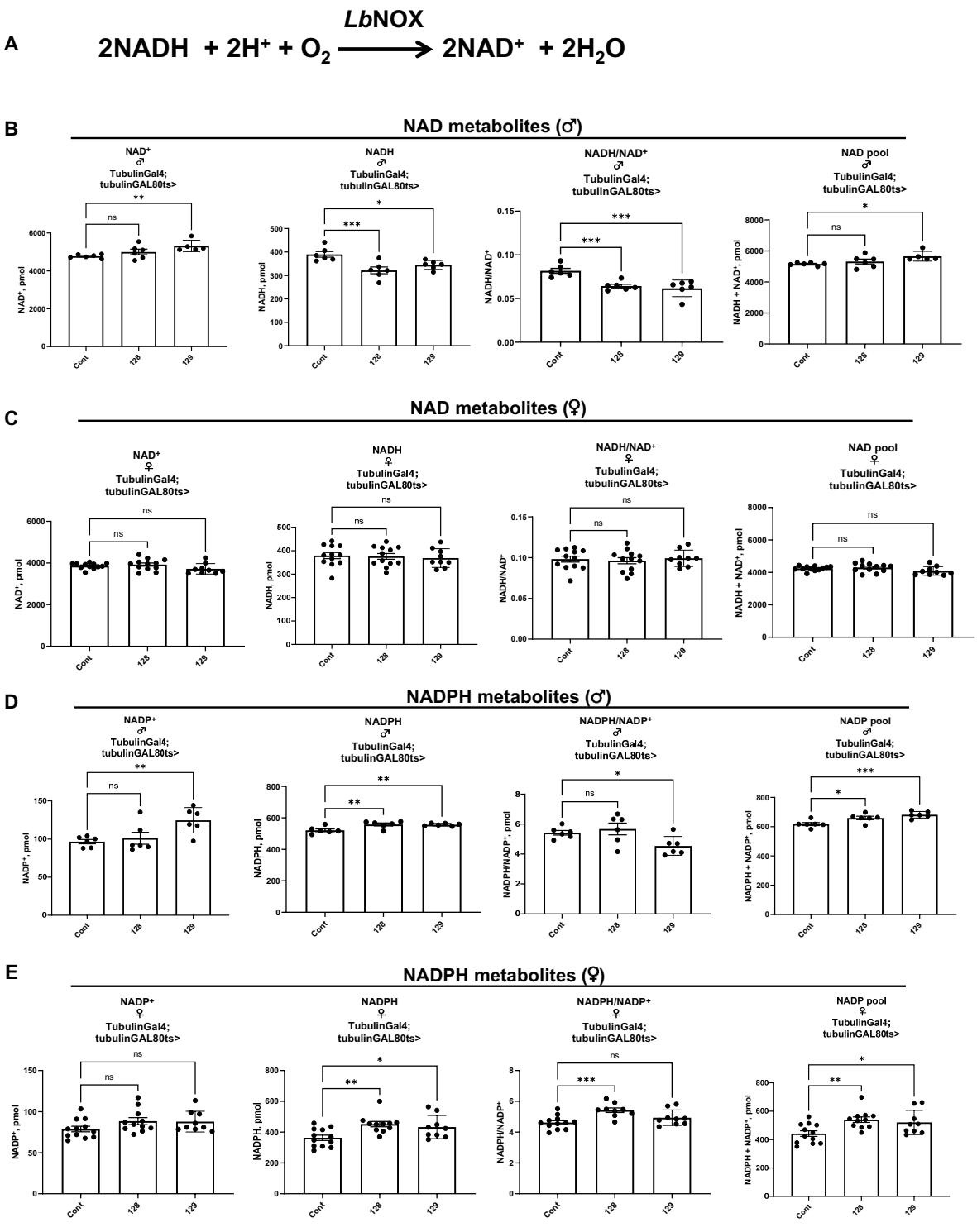

Fig. 1. *Lb*NOX expression alters NAD(P)H/NAD(P)$^+$ ratios in *Drosophila* in a sex-dependent manner. (**A**) Schematic showing the chemical reaction catalyzed by *Lb*-NOX enzyme. (**B**) Levels of different NAD metabolites measured in 1-week-old male flies expressing *Lb*NOX in the two independent lines 128 and 129. (**C**) Levels of different NAD metabolites measured in 1-week-old female flies expressing *Lb*NOX in the two independent lines 128 and 129. (**D**) Levels of different NADP metabolites measured in 1-week-old male flies expressing *Lb*NOX in the two independent lines 128 and 129. (**E**) Levels of different NAD metabolites measured in 1-week-old male flies expressing *Lb*NOX in the two independent lines 128 and 129. Values indicated in (B) to (E) are from individual biological replicates having 10 flies each. The statistical significance indicated for (B) to (E) represents a one-way analysis of variance (ANOVA) followed by uncorrected Fisher's Least Significant Difference (LSD) test. The error bars in (B) to (E) represent means ± SD. The full genotype of flies is as follows: "cont" is *tubulinGAL80^{ts}/+*, *tubulinGal4/control*; "128" is *tubulinGAL80^{ts}/UAS-LbNOX128*, *tubulinGal4/+*; and "129" is *tubulinGAL80^{ts}/+*, *tubulinGal4/UAS-LbNOX 129*. ns, not significant. *$P \leq 0.05$, **$P \leq 0.01$, ***$P \leq 0.001$.

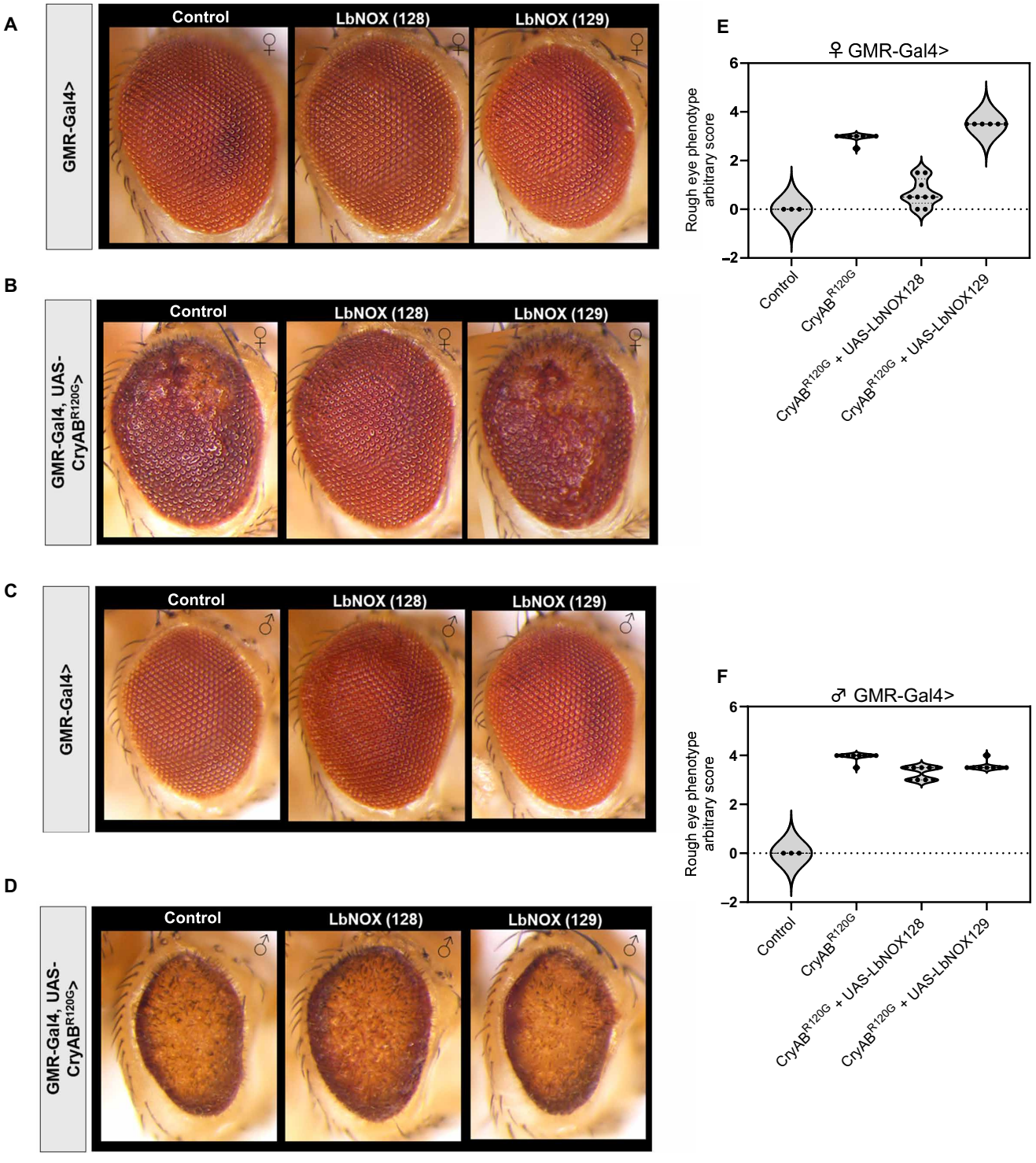

Fig. 2. *Lb*NOX expression rescues neurodegeneration associated with CryAB-induced reductive stress in female flies in a sex-dependent manner. Representative bright-field images of *Drosophila* compound eye in (**A**), female flies expressing control and *Lb*NOX line 128 and 129 using GMR-Gal4. (**B**) Female flies expressing the CryAB^{R120G} along with the control and *Lb*NOX line 128 and 129 using GMR-Gal4. (**C**) Male flies expressing control and *Lb*NOX line 128 and 129 using GMR-Gal4. (B) Male flies expressing the CryAB^{R120G} along with the control and *Lb*NOX line 128 and 129 using GMR-Gal4. (**E** and **F**) Quantification of the rough eye phenotype in female and male flies expressing CryAB^{R120G} and *Lb*NOX as indicated in the genotype. Each data point represents an individual fly scored. A total of six to nine flies were scored for each genotype. The statistical significance indicated for (E) and (F) represents one-way ANOVA with Dunnett's post hoc test. The error bars represent SEM. The full genotype of flies expressing *Lb*NOX in (A) is *GMR-Gal4/UAS-LbNOX 128* and *GMR-Gal4/UAS-LbNOX 129*. The full genotype of flies expressing *Lb*NOX in (B) is *GMR-Gal4,UAS-CryAB^{R120G}/UAS-LbNOX 128* and *GMR-Gal4,UAS-CryABR120G; UAS-LbNOX 129/+*.

appeared to rescue the reduced eye size in male flies but did not rescue the neuronal death (Fig. 2D). We quantified the rough eye phenotype using a semiquantitative approach, scoring the presence or absence of specific visual parameters, summarized in (Fig. 2, E and F).

Our data suggest that the minor differences observed between the two *Lb*NOX transgenic lines in their effects on total levels of NAD(P)(H) nicotinamide dinucleotides may have a strong impact on the functional outcome as we observed in a model of reductive stress. Notably, female flies showed a unique capacity to buffer NADH/NAD^+ ratio as despite expression of *Lb*NOX, no decrease in the NADH/NAD^+ ratio was observed in females from *Lb*NOX lines 128 and 129.

*Lb*NOX expression protects against the detrimental effects of oxidative stress

We further tested how different stress conditions (starvation, oxidative stress, or aging used as a model of integrative stress) affect levels of NAD(P)(H) nicotinamide dinucleotides and their ratios in whole flies and whether *Lb*NOX expression can modify these changes and increase survival of flies under these conditions. We placed 1-week-old control female flies on food containing only 1% agar (for inducing starvation stress) or food containing 1% agar with 5% of sucrose and 10 mM of methyl viologen dichloride hydrate (paraquat) (redox cycler that induces oxidative stress) (*24*). We also aged flies for 3 weeks at 29°C as an additional stress condition (aging, in this case). Both starvation and oxidative stress dramatically reduced NADH levels, as well as the NADH/NAD^+ ratio, with no effect on the NAD^+ levels or the total NAD pool (Fig. 3, A to C, and fig. S2A). All three stress conditions substantially decreased NADPH levels and the total NADP pool, except for aging, which did not affect the total NADP pool (Fig. 3, D to F, and fig. S2B).

To test whether *Lb*NOX expression restores the decreased NADH and NADPH levels and the decreased NADH/NAD^+ and NADPH/$NADP^+$ ratios in flies under oxidative stress, we placed 1-week-old control or *Lb*NOX-expressing female flies on food containing 1% agar with 5% sucrose and 10 mM of paraquat and compared NAD(H) and NADP(H) levels, as well as NADH/NAD^+ and NADPH/$NADP^+$ ratios, to control flies kept on a standard diet. We observed that expression of *Lb*NOX partially rescued the alterations associated with the oxidative stress for both NAD(P)H levels and NAD(P)H/$NAD(P)^+$ ratios (fig. S2, C to F). It is quite remarkable that while *Lb*NOX biochemically catalyzes the conversion of NADH to NAD^+, its expression in combination with oxidative stress (induced by paraquat) substantially increases both NAD(P)H levels and NAD(P)H/$NAD(P)^+$ ratios, suggesting that a productive rebalancing between the NAD and NADP pools might underlie the observed antioxidant response.

We next explored how *Lb*NOX expression affects the survival of flies under oxidative stress or starvation stress. *Lb*NOX expression significantly improved the survival of female flies under oxidative stress (Fig. 3G) with a moderate effect in male flies (fig. S2G). Under starvation condition, we observed only a minor effect of *Lb*NOX expression on the survival of female flies with no effect on male flies (Fig. 3H and fig. S2H). To avoid the potential contribution from experimental artifacts associated with the Gal4/$Gal80^{ts}$ system and the differences in the genetic background of the flies, we used inducible GS Gal4/UAS expression system (*25*, *26*), where UAS-transgene expression is driven by Gal4 when flies are fed mifepristone (RU486). We used Daughterless-GS (Da-GS-Gal4) to drive expression of a control parental line and *Lb*NOX line 128 and tested the ability of these flies to withstand oxidative stress after 10 days of feeding the drug RU486 (referred to as RU in figures) or ethanol (EtOH, the vehicle control). We did not observe any difference in the response of flies expressing control line across ethanol or RU treated flies (Fig. 3I). Flies expressing *Lb*NOX line 128 that were fed RU486 showed significant and robust resistance to oxidative stress compared to flies fed ethanol (Fig. 3J). In summary, we demonstrate that *Lb*NOX expression, despite promoting NADH consumption, can counteract the detrimental effects of oxidative stress by robustly boosting both NAD(P)H levels and NAD(P)H/$NAD(P)^+$ ratios.

*Lb*NOX expression prolongs *Drosophila* lifespan in a sex-dependent manner

We further sought to evaluate the effects of *Lb*NOX expression on lifespan using both the 128 and 129 lines. For lifespan analysis, we preferred to use the GS-Gal4 system to be able to perform the experiment at the ideal rearing temperature for flies (i.e., 25°C). Expression of *Lb*NOX 128 line significantly extended lifespan in female flies using two different ubiquitous GS Gal4 drivers: Da-GS-Gal4 and Actin-GS (Actin-GS-Gal4) (Fig. 4, A and C). *Lb*NOX 128 expression extended lifespan by 17.9% ($P < 0.0001$, log-rank test) under Da-GS-Gal4 and by 16.3% ($P < 0.0001$, log-rank test) with Actin-GS-Gal4. In males, *Lb*NOX 128 expression did not have a significant effect on lifespan under Da-GS-Gal4 ($P = 0.1947$, log-rank test) and extended lifespan by 6% under Actin-GS-Gal4 ($P = 0.0081$, log-rank test) (Fig. 4, B and D). *Lb*NOX 129 expression extended lifespan by 7.7% under Da-GS-Gal4, but the effect was not statistically significant ($P = 0.8332$, log-rank test) in females, whereas its expression did not affect lifespan in males (Fig. 4, E and F). *Lb*NOX 129 expression extended lifespan by 3.1% under Actin-GS-Gal4, but the effect was not statistically significant ($P = 0.5842$, log-rank test) in females, while its expression significantly decreased lifespan by 3.1% in males ($P = 0.0086$, log-rank test) (Fig. 4, G and H). In summary, we demonstrate that ubiquitous *Lb*NOX expression extends *Drosophila* lifespan in a sex-dependent manner.

NAD precursor supplementations do not further extend lifespan of *Drosophila* expressing *Lb*NOX ubiquitously

We further tested whether the effects of ubiquitous *Lb*NOX expression are comparable to those of supplementation with the common NAD precursors nicotinamide riboside (NR) and nicotinamide mononucleotide (NMN) based on NAD(P)(H) levels and NAD(P)H/$NAD(P)^+$ ratios in whole flies. Supplementation of NMN has previously been shown to significantly rescue the shortened lifespan in a *Drosophila* model of Werner syndrome (*27*). Similarly, supplementation of NR significantly rescues impaired muscle function in a *Drosophila* model of Barth syndrome (*28*). We first supplemented control flies with either NR (100 μM or 1 mM) or NMN (100 μM) for 7 days and measured the levels of NAD(H) and NADP(H) coenzymes in whole flies. In these experiments, we used only female flies as the beneficial effect of *Lb*NOX expression in the model of reductive stress was observed exclusively in females. Supplementation with either NR or NMN increased levels of NAD^+ as well as the total NAD pool and promoted a robust prooxidative shift (a decrease) in

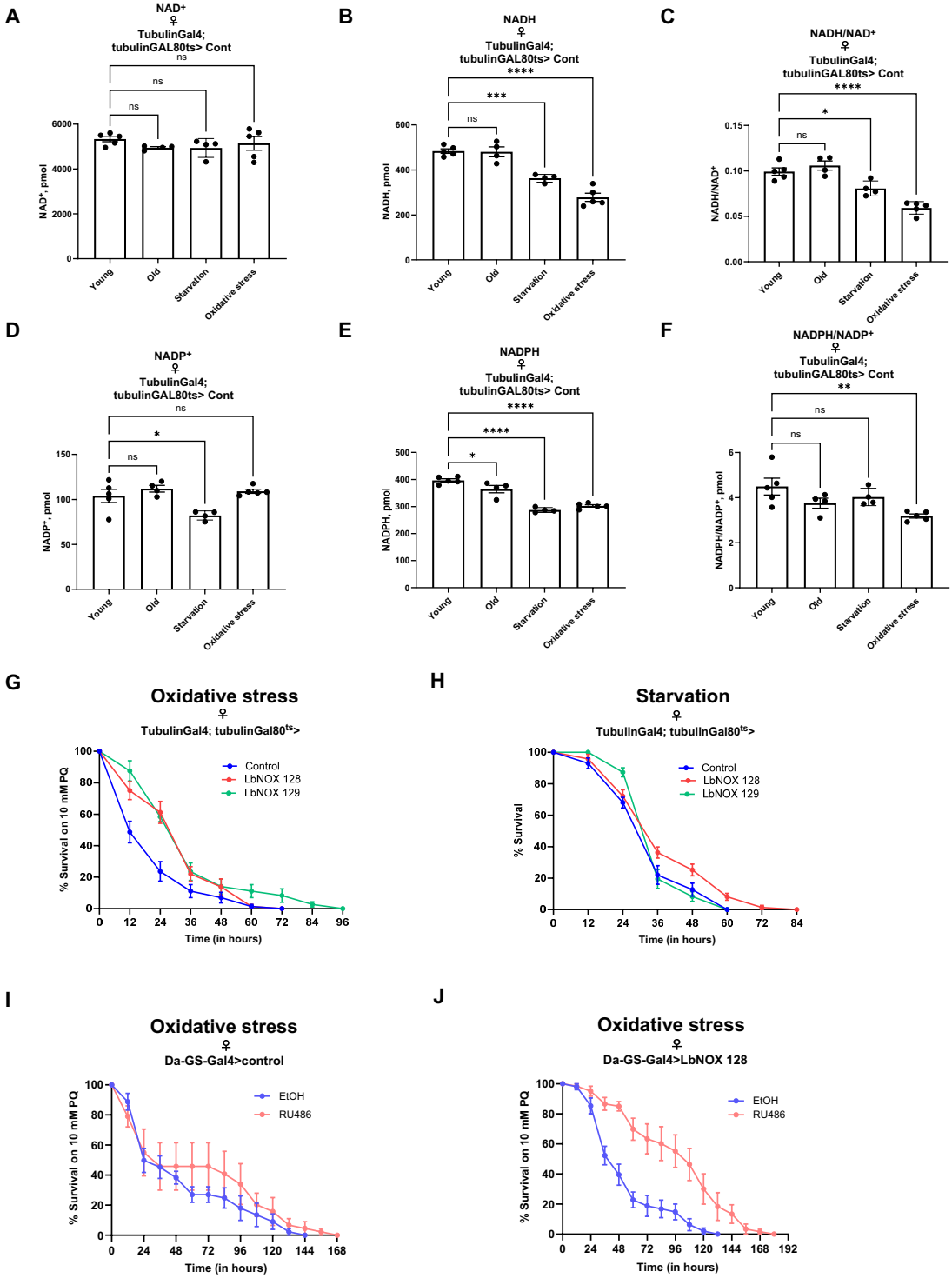

Fig. 3. *Lb*NOX expression protects against detrimental effects of oxidative stress. Levels of NAD^+ (**A**), NADH (**B**), and NADH/NAD^+ ratios (**C**) in female flies that were 1 week old (young), 3 weeks old (old), and subjected to starvation or oxidative stress for 16 hours. Levels of $NADP^+$ (**D**), NADPH (**E**), and NADPH/$NADP^+$ ratios (**F**) in female flies that were 1 week old (young), 3 weeks old (old), and subjected to starvation or oxidative stress for 16 hours. Survival of 1-week-old female flies expressing either attp2 (control) or *Lb*NOX ubiquitously with the tubulin-Gal4 driver when subjected to oxidative stress (**G**) or starvation stress (**H**). Survival of 1-week-old female flies expressing either control or *Lb*NOX line 128 ubiquitously with the Da-GS-Gal4 driver when subjected to oxidative stress (**I**) or starvation stress (**J**). Values indicated in (A) to (F) are from independent biological replicates having 10 flies each. The statistical significance indicated for (A) to (F) represents a one-way ANOVA followed by uncorrected LSD test. The error bars in (A) to (F) represent means ± SD. The error bars in (G) to (J) represent means ± SEM. Total number of flies tested per genotype in (G) to (J) are six independent replicates with 12 flies each ($N = 72$). The full genotype of flies expressing *Lb*NOX in (G) and (H) is *tubulinGAL80^{ts}/UAS-LbNOX128; tubulinGal4/$^+$*, and *tubulinGAL80^{ts}/$^+$; tubulinGal4/UAS-LbNOX129*. The full genotype of flies in (I) is *Da-GS-Gal4/control*, and in (J) is *UAS-LbNOX128/$^+$; Da-GS-Gal4/$^+$*. $^*P \leq 0.05$, $^{**}P \leq 0.01$, $^{***}P \leq 0.001$, $^{****}P < 0.0001$.

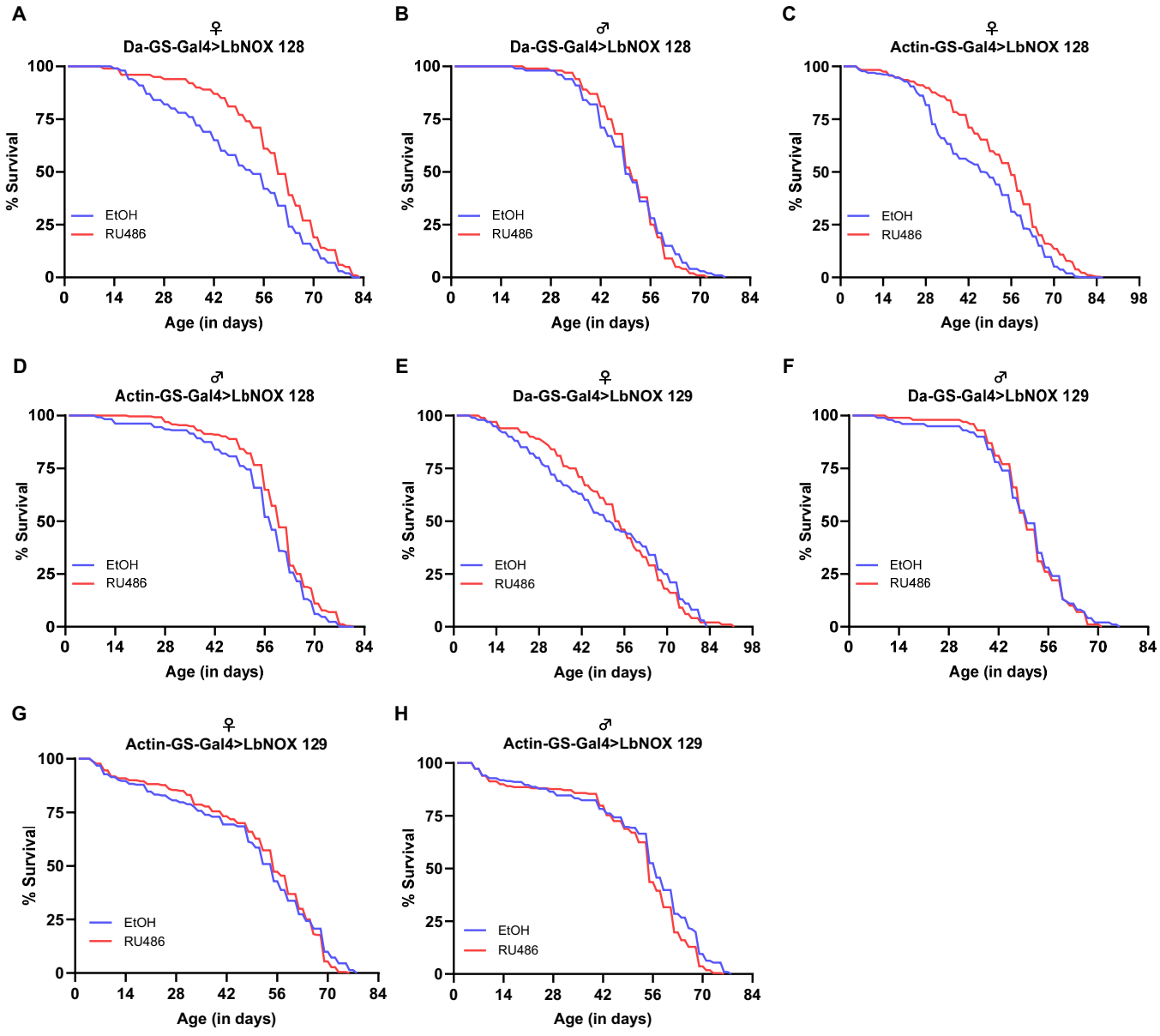

Fig. 4. *Lb*NOX expression prolongs *Drosophila* lifespan in a sex-dependent manner. (**A**) Ubiquitous adult-onset expression of *Lb*NOX 128 with Da-GS-Gal4 increases lifespan in females. $P < 0.0001$. (**B**) Ubiquitous adult-onset expression of *Lb*NOX 128 with Da-GS-Gal4 does not affect lifespan in males. $P = 0.1947$. (**C**) Ubiquitous adult-onset expression of *Lb*NOX 128 with actin-GS-Gal4 increases lifespan in females. $P < 0.0001$. (**D**) Ubiquitous adult-onset expression of *Lb*NOX 128 with actin-GS-Gal4 increases lifespan in males. $P = 0.0081$. (**E**) Ubiquitous adult-onset expression of *Lb*NOX 129 with Da-GS-Gal4 does not affect lifespan in females. $P = 0.8332$. (**F**) Ubiquitous adult-onset expression of *Lb*NOX 129 with Da-GS-Gal4 does not affect lifespan in males. (**G**) Ubiquitous adult-onset expression of *Lb*NOX 129 with actin-GS-Gal4 does not affect lifespan in females. $P = 0.5842$. (**H**) Ubiquitous adult-onset expression of *Lb*NOX 129 with actin-GS-Gal4 decreases lifespan in males. $P = 0.0086$. [(A) to (H)] For each genotype, a population of 230 to 300 flies were analyzed across 10 to 11 independent replicates. EtOH refers to ethanol and was used as a vehicle control for the drug supplementation. RU refers to the drug RU486. The full genotype of flies expressing *Lb*NOX in (A) and (B) is *UAS-LbNOX128/+; Da-GS-Gal4/+*, in (C) and (D) is *Actin-GS-Gal4/UAS-LbNOX 128,* in (E) and (F) is *UAS-LbNOX 129/Da-GS-Gal4*, and in (G) and (H) is *Actin-GS-Gal4/+; UAS-LbNOX 129/+*.

NADH/NAD^+ ratio (Fig. 5, A to C, and fig. S3A). In contrast, only supplementation with NMN increased $NADP^+$ levels (with no significant effect on the total NADP pool) and decreased NADPH/$NADP^+$ ratio (Fig. 5, D to F, and fig. S3B). We did not observe any significant differences between the two NR concentrations tested.

We further tested how supplementation of nicotinic acid (NA), β-hydroxybutyrate (BHB), and *N*-acetyl-cysteine (NAC) affected levels of NAD(H) and NADP(H) coenzymes in whole flies. NA has previously been shown to increase the intracellular NAD levels in Hs68 cells and *Caenorhabditis elegans* (*C. elegans*), as well as to extend worm's lifespan (*29*). In *Drosophila*, expression of *Drosophila* nicotinamidase (D-NAAM/NAMase) converts nicotinamide to NA, which decreases NADH/NAD^+ levels and extends lifespan (*30*). BHB is a circulating ketone body, which is metabolized into acetoacetate by

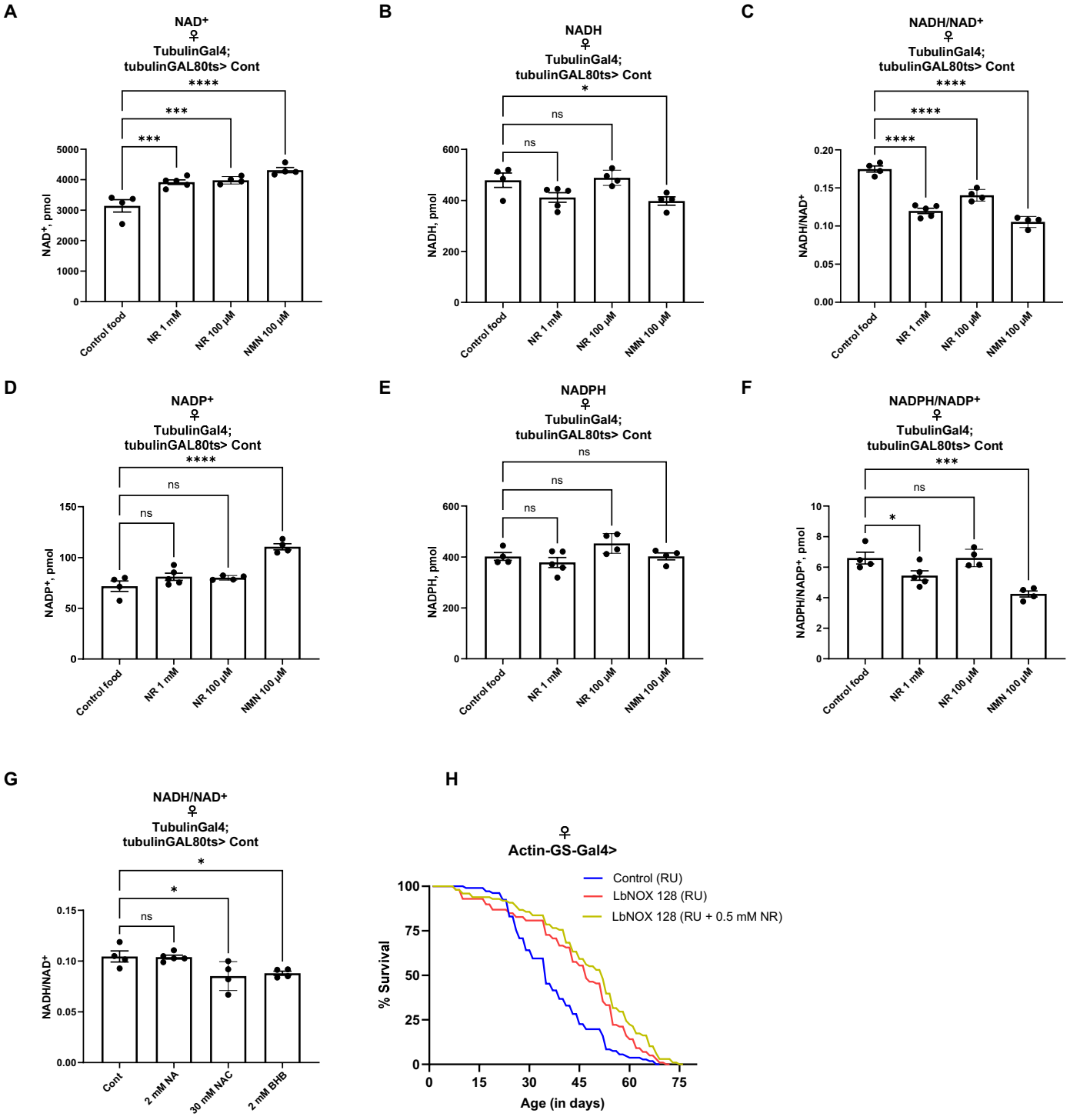

Fig. 5. NAD precursor supplementations do not further extend lifespan of *Drosophila* expressing *Lb*NOX ubiquitously. Levels of NAD^+ (**A**), NADH (**B**), and NADH/NAD^+ ratios (**C**) in female control flies fed with food containing 1 mM NR, 100 µM NR, or 100 µM NMN compared to flies fed on control food. Levels of $NADP^+$ (**D**), NADPH (**E**), and NADPH/$NADP^+$ ratios (**F**) in female control flies fed with food with 1 mM NR, 100 µM NR, or 100 µM NMN. (**G**) The NADH/NAD^+ ratio in female control flies fed with food containing 2 mM NA, 30 mM NAC, or 2 mM BHB compared to flies fed on control food. (**H**) Ubiquitous adult-onset expression of *Lb*NOX 128 with actin-GS-Gal4 increases lifespan in females that is not further extended with 0.5 mM NR supplementation. For each genotype, a population of 100 to 110 flies were analyzed across five to six independent replicates. RU, 200 µM RU486 and NR, 0.5 mM of drug NR. Values indicated in (A) and (G) are from independent biological replicates having 10 flies each. The statistical significance indicated for (A) to (G) represents a one-way ANOVA followed by uncorrected Fisher's LSD test. The error bars in (A) to (G) represent means ± SD. The full genotype of flies in (A) to (G) is *tubulinGAL80^{ts}/+; tubulinGal4/control*, and in (H) is *tubulinGAL80ts /UAS-LbNOX128; tubulinGal4/+*. $^*P \leq 0.05$, $^{**}P \leq 0.01$, $^{***}P \leq 0.001$.

BHB dehydrogenase 1 in mitochondria of target tissues, thereby generating NADH. In humans, food supplementation with BHB or sodium butyrate has been associated with multiple health benefits (*31*). Last, NAC is associated with lifespan benefits across different species (*1*) and may indirectly affect NAD(P) pools by acting as an antioxidant. We found that supplementation of 2 mM NA did not affect NADH/NAD$^+$ or NADPH/NADP$^+$ ratios in *Drosophila* (Fig. 5G and fig. S3, C to G). However, supplementation of 30 mM NAC or 2 mM BHB significantly (but less potently than NR or NMN) decreased NADH/NAD$^+$ without affecting the NADPH/NADP$^+$ ratio (Fig. 5G and fig. S3, C to G).

As NR significantly decreased NADH/NAD$^+$ ratio (Fig. 5C) and *Lb*NOX expression significantly increased the NADP pool (Fig. 1E) and prolonged lifespan (Fig. 4C) in female flies, we further tested whether the combination of NR supplementation and *Lb*NOX expression would be more efficient than *Lb*NOX expression alone. In female flies, supplementation of 0.5 mM NR along with *Lb*NOX expression did not significantly extend lifespan compared to *Lb*NOX expression alone (Fig. 5H). In summary, we assessed how different NAD boosters or modulators (NR, NMN, NA, BHB, and NAC) affect NAD metabolism in *Drosophila* and demonstrated that the lifespan extension achieved via *Lb*NOX expression cannot be further extended with NR supplementation.

*Lb*NOX expression reprograms *Drosophila* metabolism with a strong impact on de novo NAD biosynthesis

To better understand the mechanism of lifespan extension by *Lb*NOX expression, we performed metabolomic profiling on either control flies or two different *Lb*NOX-expressing lines under the control of the ubiquitous temperature-sensitive (*tubulin-Gal4* and *tubulin-Gal80^{ts}*) driver after 7 days of expression (Fig. 6, A to C, and table S1). Principal components analysis of the measured metabolites clearly distinguished control flies from *Lb*NOX lines 128 and 129 (fig. S4). We identified 70 metabolites that were significantly altered in the *Lb*NOX 128 line, and 19 metabolites were significantly altered in the *Lb*NOX 129 line, while 18 metabolites were significantly and commonly changed in both *Lb*NOX lines (Fig. 6D). To understand which metabolic pathways were among the most significantly changed by *Lb*NOX expression, we applied Metabolite Set Enrichment Analysis. We found that the tricarboxylic acid (TCA) cycle and tryptophan metabolism were among the metabolic pathways most affected by *Lb*NOX expression (Fig. 6, E and F, and table S2. *Lb*NOX expression dramatically altered the levels of several metabolites (tryptophan, kynurenine, kynurenic acid, quinaldic acid, tryptamine, indole-3-acetic acid, indole-3-carboxylic acid, and indoleacetic acid) in the tryptophan metabolic pathway that are involved in de novo NAD biosynthesis (Fig. 6, G and H). We also noted that *Lb*NOX expression in both lines 128 and 129 robustly decreased levels of metabolites attributed to the indole pyruvate pathway, which is typically linked to tryptophan and kynurenine metabolism (*32*–*36*). The results of our metabolomic profiling may explain the stronger effects of *Lb*NOX expression on cellular metabolism in the 128 line. In addition, increase in the NADP pool under *Lb*NOX expression may be explained by the up-regulation of NAD de novo biosynthesis [e.g., NAD$^+$ subsequently is converted to NADP$^+$ by NAD kinase (NADK)] and depletion of metabolites in the tryptophan metabolic pathway.

Muscle-specific *Lb*NOX expression protects against oxidative stress and improves neuromuscular function at old age

Ubiquitous *Lb*NOX expression protected against oxidative stress with a negligible effect on starvation resistance. Since NAD metabolism may play different roles across tissues, we used our genetic tool to test the impact of tissue-specific *Lb*NOX expression. We expressed it in two metabolically active tissues—muscles and neurons. *Lb*NOX was expressed in adult muscles using the *Dmef-Gal4*, *tubulin-Gal80^{ts}*, or in neuronal tissues using the *Elav-Gal4, tubulin-Gal80^{ts}* temperature-inducible system. Muscle-specific *Lb*NOX expression significantly enhanced resistance to oxidative stress in female flies (Fig. 7A) compared to that conferred by ubiquitous expression, while no beneficial effect was observed in male flies (Fig. 7B). We also observed significant resistance to starvation stress in both female and male flies expressing the line 128 (fig. S5, A and B). Pan-neuronal *Lb*NOX expression did not affect resistance to oxidative stress in female flies (Fig. 7C), while it was detrimental in male flies (Fig. 7D). We also observed that pan-neuronal *Lb*NOX expression did not affect resistance to starvation stress in both female and male flies (fig. S5, C and D).

The beneficial effects of expressing *Lb*NOX in muscles, compared to neurons, led us to explore the impact of muscle-specific *Lb*NOX expression on lifespan and neuromuscular health during aging. Although using a GS line is the gold standard for aging-related studies, Poirier *et al.* (*37*) tested several major GS drivers for their expression without an inducer and found leakiness associated with the myosin heavy chain GS line (MHC-GS-Gal4) in the thoracic flight muscles and leg muscles of the flies. Robles-Murguia *et al.* (*38*) generated a new GS Gal4 driver for drug-induced transgene expression in flight muscles, Act88F-GS, which did not drive significant transgene expression in the absence of RU486. However, they found that RU486 represses the expression of nuclear-encoded mitochondrial genes and reduces the activity of succinate dehydrogenase. As all these findings could potentially complicate the interpretation of muscle-specific *Lb*NOX expression using the muscle-specific GS system, we performed all our experiments using the *Dmef-Gal4*, *tubulin-Gal80^{ts}* line. We found a significant extension of lifespan in flies expressing *Lb*NOX with Dmef-Gal4 (Fig. 7, E and F). The beneficial effects were also observed in male flies. We tested the climbing ability of flies as a proxy for neuromuscular health at different ages and found that flies expressing *Lb*NOX only in muscles exhibited significantly higher climbing ability compared to control flies, particularly at older ages (Fig. 7, G and H). Again, this beneficial effect was observed in both male and female flies. Overall, these results highlight the tissue-specific impact of modulating NADH consumption, which differs from effects observed through whole-body manipulations.

Tissue-specific *Lb*NOX expression improves sleep profiles in aged flies back to a youthful state

Recent studies have shown the importance of NAD(P) metabolism in the regulation of sleep in *Drosophila* (*39*, *40*), mice (*41*, *42*), and humans (*43*, *44*). As the key genes regulating circadian rhythm have been identified (*45*) and are conserved from flies to humans (*46*, *47*), *Lb*NOX represents a unique tool to dissect the role of NAD(P) metabolism across different tissues and populations of cells. Sleep is defined in *Drosophila* as a prolonged period of immobility longer than 5 min (*48*) and can be measured using the

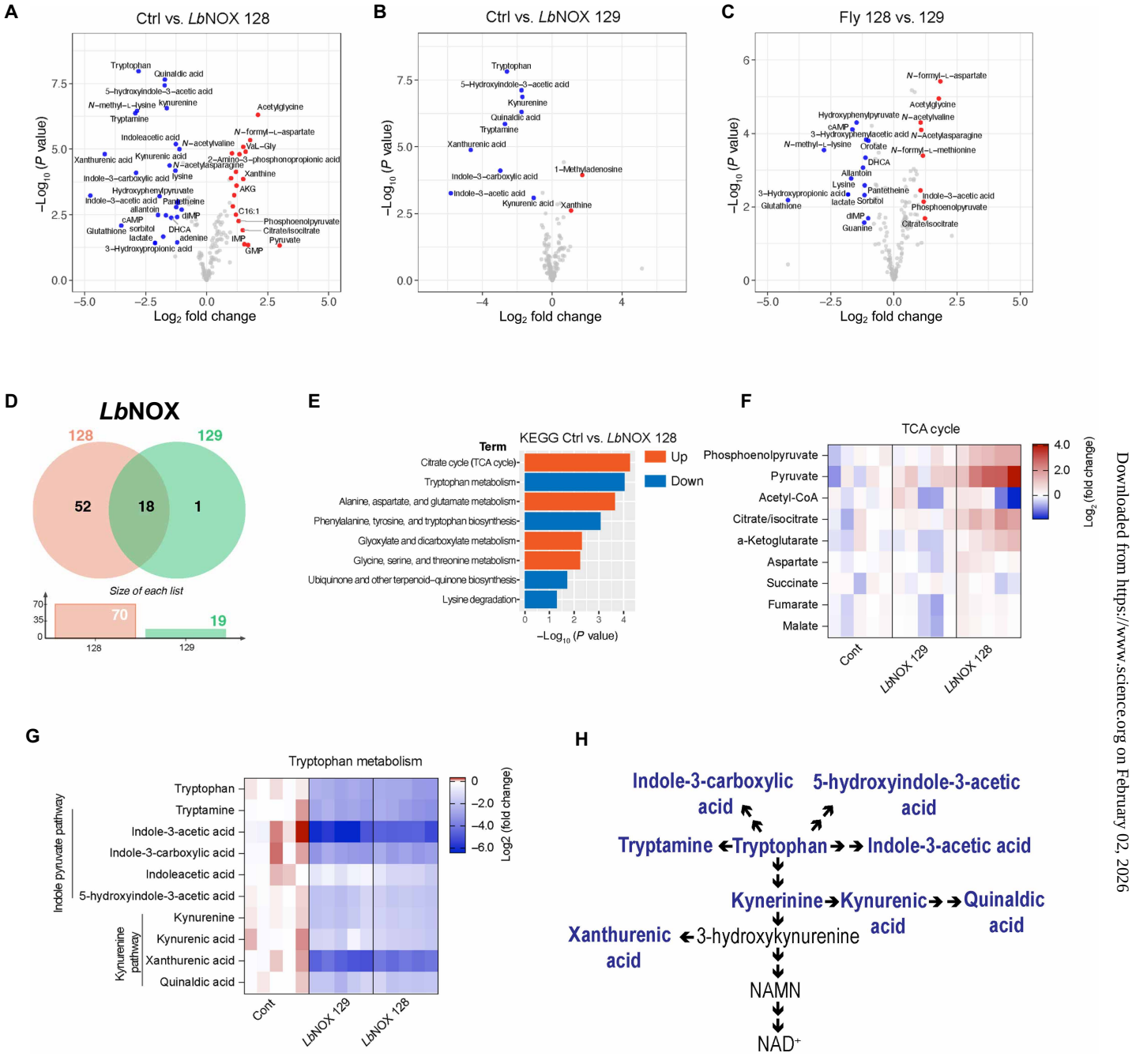

Fig. 6. *LbNOX* expression reprograms *Drosophila* metabolism with a strong impact on de novo NAD biosynthesis. Volcano plots of targeted metabolomics of female *Drosophila* *Lb*NOX lines 128 (**A**) and 129 (**B**) relative to controls as well as comparison between 128 and 129 lines (**C**). Accumulated metabolites are shown in red dots, decreased metabolites are shown in blue dots, and gray dots represent statistically nonsignificant changes. The statistical significance for (A) to (C) represents *P* value cutoff = 0.05, fold change cutoff = 0.5. (**D**) Venn diagrams of metabolites significantly altered in *Lb*NOX expression lines 128 and 129. (**E**) Kyoto Encyclopedia of Genes and Genomes (KEGG) pathways analysis based on MetaboAnalyst platform for metabolites with *Lb*NOX expression line 128 relative to controls. Orange and blue depict pathways that are up-regulated or down-regulated, respectively (based on the abundance of the corresponding metabolites). Heatmaps of the most affected metabolites of TCA cycle (**F**) and tryptophan metabolism and indole pyruvate pathway (**G**) in female *Lb*NOX lines 128 and 129. In heatmaps [(F) and (G)], each column represents a biologically independent sample. (**H**) A simplified schematic of the kynurenine and indole pyruvate pathways in *Drosophila*. Two consecutive arrows assume multiple reaction steps. Metabolites from the heatmap (G) are in blue color. The full genotype of flies is as follows: cont or ctrl is *tubulinGAL80^{ts}/$^{+}$; tubulinGal4/control*, 128 is *tubulinGAL80^{ts}/UAS-LbNOX128; tubulinGal4/$^{+}$*, and 129 is *tubulinGAL80^{ts}/$^{+}$; tubulinGal4/UAS-LbNOX 129*.

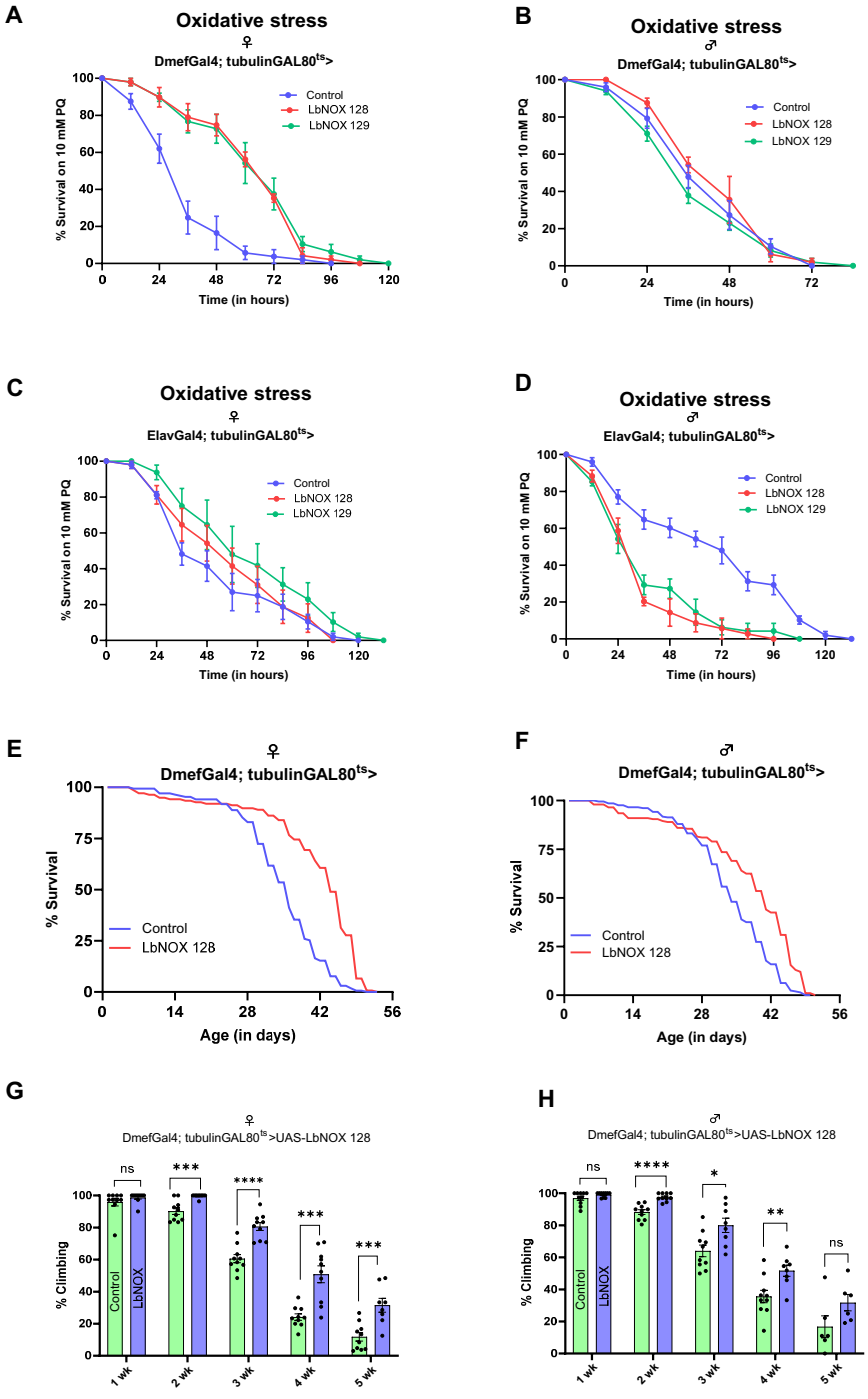

Fig. 7. Muscle-specific *Lb*NOX expression efficiently protects against oxidative stress and supports muscle health in old age. Survival of female (**A**) and male (**B**) control flies and flies with muscle-specific *Lb*NOX expression under oxidative stress. Survival of female (**C**) and male (**D**) control flies and flies with neuron-specific *Lb*NOX expression under oxidative stress. (**E**) Muscle-specific adult-onset expression of *Lb*NOX #128 with Dmef-Gal4 increases lifespan in females ($P < 0.001$, log-rank test) ($N = 170$ flies for control; $N = 137$ flies for *Lb*NOX). (**F**) Muscle-specific adult-onset expression of *Lb*NOX #128 with Dmef-Gal4 increases lifespan in males ($P < 0.001$, log-rank test) ($N = 208$ flies for control; $N = 200$ flies for *Lb*NOX). (**G** and **H**) Climbing ability of female and male flies expressing LbNOX #128 with Dmef-Gal4 compared to control flies at mentioned ages, respectively. A total of 120 flies were tested that were spread across 10 independent replicates. For data shown in (A) to (D), a total of 50 flies were tested for each genotype that were spread across four independent replicates. The full genotype of flies expressing *Lb*NOX in (A), (B), and (E) to (H) is *tubulinGAL80^{ts}/UAS-LbNOX128; DmefGal4/$^{+}$*, and *tubulinGAL80^{ts}/$^{+}$; DmefGal4/UAS-LbNOX129*, and in (C) to (D) is *ElavGal4/$^{+}$; tubulinGAL80ts/UAS-LbNOX128*. The error bars in (A) to (D), (G), and (H) represent SEM. The statistical significance indicated in (G) and (H) represents unpaired two-tailed Student's *t* test. wk, week/weeks. $^{*}P \leq 0.05$, $^{**}P \leq 0.01$, $^{***}P \leq 0.001$, $^{****}P < 0.0001$.

Drosophila activity monitors (DAMs) by determining the number and duration of sleep bouts.

Because we found the beneficial effects of *Lb*NOX selectively in female flies, we monitored sleep in control female flies aged from 1 to 5 weeks. We found that aging is associated with disruption of multiple sleep parameters, namely sleep profile, average total sleep, sleep bout length, and bout number. These changes first appeared at 3 weeks of age at 29°C and persisted thereafter (Fig. 8, A to D). We observed a significant change in the sleep profile at 3 weeks compared to 1 week (Fig. 8A). In control flies (*tubulin-Gal4, tubulin-Gal80^{ts}* crossed to the parental line), aging was associated with an increase in average total sleep (Fig. 8B), which was accompanied by an increase in bout length (Fig. 8C) and a decline in bout number (Fig. 8D). We further tested whether whole-body *Lb*NOX expression could rescue the aging-associated disruption of the sleep profile. We found that ubiquitous expression of *Lb*NOX line 128 significantly rescued the average sleep profile in 3-week-old flies (Fig. 8E). It also rescued the disrupted total sleep, sleep bout length, and sleep bout number in aged flies (Fig. 8, F to H).

Sleep is known to be regulated by neuronal inputs; hence, we tested whether neuron-specific *Lb*NOX expression could also rescue aging-associated sleep deficits. We expressed *Lb*NOX using the *Elav-Gal4, tubulin-Gal80^{ts}* driver, and it rescued the disrupted sleep profile in 3-week-old flies (Fig. 8I). The neuronal expression rescued the average total sleep but did not significantly alter the sleep bout number and length at old age (fig. S6, A to C). The beneficial effects observed with muscle-specific expression of *Lb*NOX on lifespan, muscle function, and stress tolerance prompted us to further test whether muscle-specific expression of *Lb*NOX could exert any beneficial effects on sleep as well. Intriguingly, expression of *Lb*NOX using the *Dmef-Gal4, tubulin-Gal80^{ts}* driver completely rescued the sleep profile in aged flies (Fig. 8J), demonstrating that tissue-specific modulation of NAD metabolism is sufficient to drive beneficial effects at the organismal level. Besides the sleep profile, it also showed rescue of the average total sleep as well as sleep bout length and number (fig. S6, D to F).

In summary, we demonstrate that utilization of *Lb*NOX allows for the assessment of tissue-specific roles of NAD metabolism in different cellular processes and its impact on overall health and lifespan in *Drosophila*. Furthermore, we provide evidence that modulation of muscle-specific metabolism is sufficient to restore aging-associated sleep deficits.

DISCUSSION

Exploiting xenotopic tools to manipulate metabolism

In recent years, manipulations of over a hundred different metabolic enzymes have been shown to prolong lifespan in different organisms (*1*). However, targeting only species-specific enzymes may not be sufficient to reverse age-dependent changes in a particular metabolic pathway and will only partially reverse age-dependent processes. An alternative approach to targeting an organism's own enzymes is to bring a novel function from other species (a xenotopic approach) that would resolve or reprogram a metabolic pathway in a beneficial way for an organism to achieve healthy aging (*11*). The yeast *Saccharomyces cerevisiae* NADH dehydrogenase internal 1 (NDI1) and the sea-squirt *Ciona intestinalis* alternative ubiquinol oxidase (AOX) are probably among the most commonly used xenotopic tools in *Drosophila* to study the role of the mitochondrial ETC in aging and aging-related diseases (*49*–*52*). Alternative yeast NADH dehydrogenase NDI (faces matrix) can bypass mitochondrial complex I (CI), and AOX can bypass CIII and CIV. We have previously created and tested several additional xenotopic tools including Methioninase (*53*), *Lb*NOX (*12*), TPNOX (*54*), and *Ec*STH (*55*). We created transgenic flies expressing Methioninase, a bacterial enzyme capable of degrading methionine to ammonia, α-ketobutyrate, and methanethiol, and demonstrated that either whole-body or tissue-specific Methioninase expression can dramatically extend *Drosophila* health- and lifespan and exert physiological effects associated with methionine restriction (*53*). Here, we created transgenic flies carrying the *Lb*NOX tool and demonstrated its utility in studying NAD(P) metabolism in vivo.

L. brevis water-forming NADH oxidase

Unlike other bacterial NADH oxidases, *Lb*NOX does not generate H_2O_2 and is strictly NADH specific (Fig. 1A). In our original study, *Lb*NOX was expressed in HeLa cells [both untargeted (*Lb*NOX) and mitochondria-targeted (mito*Lb*NOX) versions] to demonstrate that direct NAD^+ recycling is sufficient to restore proliferation in cells with impaired ETC activity (*12*). Currently, *Lb*NOX and mito*Lb*NOX are commonly used reagents to dissipate cytoplasmic or mitochondrial NADH pools (with a concomitant decrease in NADH/NAD^+ ratio) in settings of both dysfunctional and intact mitochondrial ETC (*11*). In males, *Lb*NOX expression resulted in a decrease in NADH levels and a concomitant decrease in NADH/NAD^+ ratio, while in both males and females, expression of *Lb*NOX resulted in both a robust increase in NADPH and the NADPH/$NADP^+$ ratio (Fig. 1, B, D, and E). These findings highlight the importance of testing xenotopic tools in vivo as results previously obtained in mammalian cell culture cannot be extrapolated to model organisms.

Moreover, *Lb*NOX can be coupled with other xenotopic tools targeting redox stress [TPNOX (*54*) or *Ec*STH (*17*, *55*)] to obtain different outcomes in NADH/NAD^+ and NADPH/$NADP^+$ ratios. Previously, we used *Drosophila* to create a complex genetic background that allowed for the simultaneous targeting of several cancer-related genes (*56*). As we have limited knowledge of tissue-specific metabolic dysregulation with aging (*57*) and how different interventions interact in extension of health- and lifespan (*58*), a similar approach can be applied to combine different xenotopic tools targeting redox stress (or other processes) to study these combinations and their effects on lifespan in vivo.

Targeting NAD metabolism to delay aging

Multiple studies in different organisms have demonstrated a decline in the total levels of NAD^+ with age in a tissue-specific manner. This has led to the hypothesis that a decline in NAD^+ levels with age is one of the major contributing factors to the aging process (*2*–*4*). Multiple preclinical studies in rodents have provided evidence for the beneficial effects of supplementation with NAD biosynthetic precursors that boost total cellular NAD levels (*7*–*10*). However, supplementation studies neither allow testing of the tissue-specific roles of restoring NAD^+ levels nor do they allow investigation of how NADH/NAD^+ ratio itself regulates the aging process. Moreover, in a systematic review of aging-related NAD changes across different organisms, the authors noted that there are no published papers that address whether NAD^+ levels decline with age in *Drosophila* model (*7*). Despite this, targeting NAD metabolism in *Drosophila* via whole-body or neuron-specific expression of D-NAAM/NAMase decreased NADH/NAD^+ ratio and extended lifespan (*30*).

By using *Lb*NOX as a genetically encoded xenotopic tool (*12*) and a binary UAS/GAL4 system (*59*), we were able to test whether

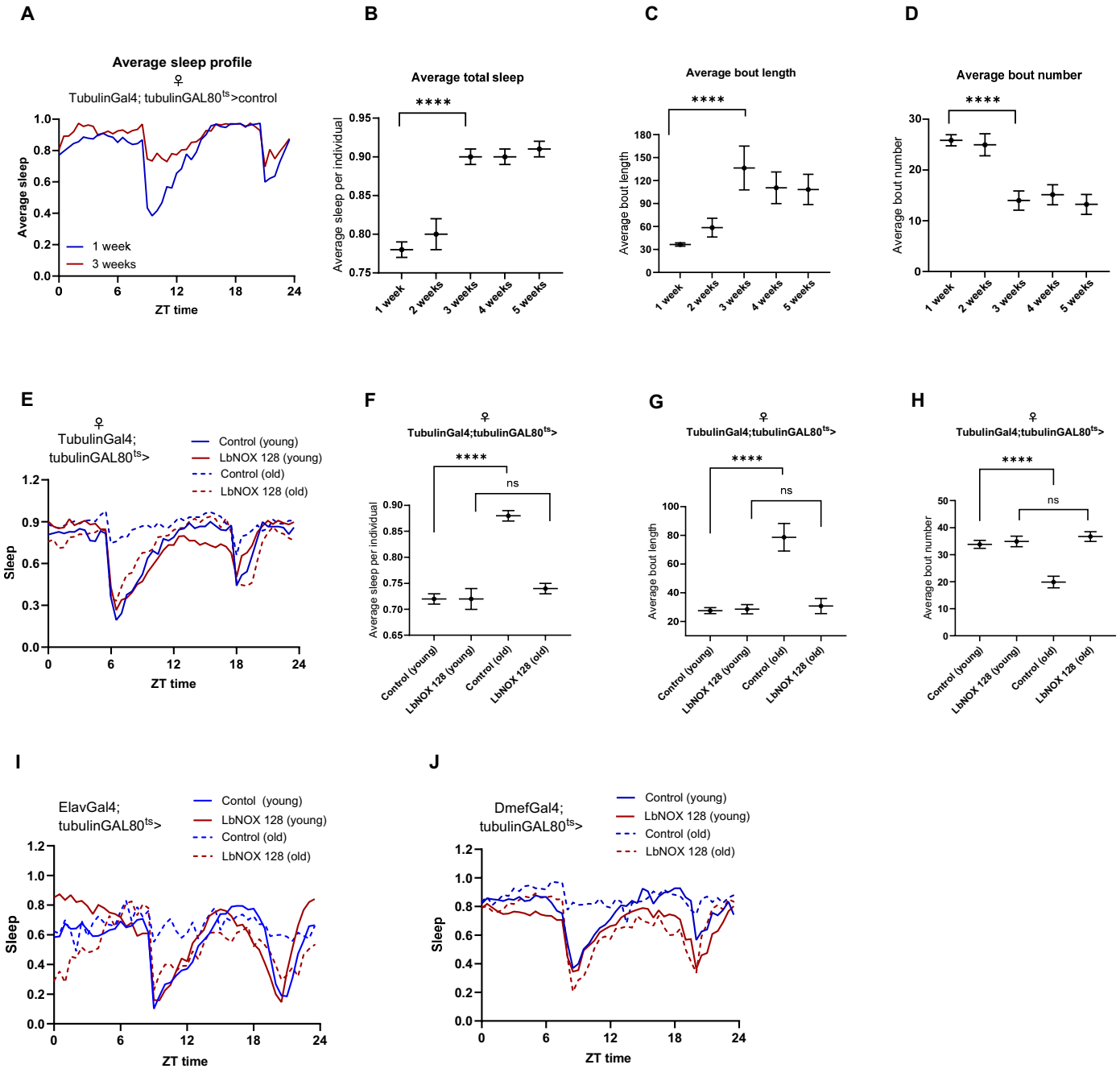

Fig. 8. Tissue-specific *Lb*NOX expression improves sleep profiles in aged flies back to a youthful state. (**A**) Average sleep profile of control flies (*tubulin-Gal4; tubulin-GAL80^{ts}* crossed to the parental line) at 1 and 3 weeks of age. ZT time refers to Zeitgeber time with respect to the onset of light. (**B**) Average total sleep of control flies of mentioned ages. (**C**) Average sleep bout length of control female flies at mentioned ages. (**D**) Average sleep bout number of control female flies at mentioned ages. (**E**) Average sleep profile of control and *Lb*NOX-expressing (line 128) female flies driven by *tubulin-Gal4; tubulin-GAL80^{ts}* at 1 week (young) and 3 weeks (old) of age. ZT time refers to Zeitgeber time with respect to the onset of light. (**F**) Average total sleep of flies of mentioned genotypes at 1 week and 3 weeks of age. (**G**) Sleep bout length of mentioned genotypes at 1 week and 3 weeks of age. (**H**) Sleep bout number of mentioned genotypes at 1 week and 3 weeks of age. (**I**) Average sleep profile of flies of control or *Lb*NOX-expressing (line 128) flies driven by *Elav-Gal4, tubulin-GAL80^{ts}* at 1 week and 3 weeks of age. (**J**) Average sleep profile of flies of control or *Lb*NOX-expressing (line 128) flies driven by *Dmef-Gal4, tubulin-GAL80^{ts}* at 1 week and 3 weeks of age. For (A) to (J), a total of 32 flies were loaded onto the DAM cassette per genotype. Analysis platform automatically removed data from flies that died during acquisition of data. Error bars represent means ± SEM; significance was determined by *t* test. The full genotype of flies in (A) to (D) is *tubulinGAL80^{ts}/+; tubulinGal4/control*, and in (E) to (H) is *tubulinGAL80^{ts} /UAS-LbNOX 128; tubulinGal4/+*, in (I) is *ElavGal4/+; UAS-LbNOX128/tubulinGAl80^{ts}*, and in (J) is *tubulinGAL80^{ts}/UAS-LbNOX128; DmefGal4/+*. *$P \leq 0.05$, **$P \leq 0.01$, ***$P \leq 0.001$, ****$P < 0.0001$.

directly manipulating NADH/NAD$^+$ ratio ubiquitously (mimicking supplementation of NAD precursors) or in a tissue-specific manner affects *Drosophila* aging. We tested how NAD levels change with age and in response to stress, identifying whether *Lb*NOX expression phenocopies supplementation of NAD precursors and whether altering NADH/NAD$^+$ ratio alone or in combination with NAD precursors prolongs lifespan. Unexpectedly, we found that NADH/NAD$^+$ and NADPH/NADP$^+$ ratios were significantly altered under stress conditions but not with aging (Fig. 3, C and F). This finding agrees with a recent study demonstrating that NADH/NAD$^+$ and NADPH/NADP$^+$ ratios do not change in mice with healthy aging because they are buffered by the activities of fatty acid desaturases that promote NAD$^+$ recycling activity (*14*). Accordingly, with an oxidative stress–induced decrease in NADH/NAD$^+$ and NADPH/NADP$^+$ ratios, we demonstrate a protective role of *Lb*NOX expression that robustly increases both ratios under stress conditions despite the NADH-consuming activity of the *Lb*NOX enzyme (fig. S2, D and F). Although we do not observe age-induced changes in NADH/NAD$^+$ and NADPH/NADP$^+$ ratios, we did observe the beneficial effects of *Lb*NOX expression on lifespan (Fig. 4, A and C). There could be several explanations for these beneficial effects. First, age-induced changes in NADH/NAD$^+$ and NADPH/NADP$^+$ ratios are not homogeneous across different tissues and may not be unidirectional. McReynolds *et al.* (*60*) used isotope tracing and mass spectrometry (MS) to probe age-related changes in NAD metabolism across tissues in aged mice. They found that the decline in NAD with healthy aging is relatively subtle and tissue dependent (for example, the reduced forms of NADH and NADPH significantly declined with age in the liver and increased in the brain) (*60*). This will result in the absence of aging-induced whole-body changes, while NAD(P) levels can be altered dramatically at the tissue-specific level. Second, age-induced changes in NAD(P) metabolism can be compensated by other metabolic pathways (*14*). Lien *et al.* (*14*) observed that levels of NAD$^+$, NADH, and the NADH/NAD$^+$ ratio were unchanged in plasma, liver, gastrocnemius muscle, and brain tissues with healthy aging; however, aging tissues, particularly the brain, exhibited evidence of up-regulated fatty acid and sphingolipid metabolism reactions that regenerate NAD$^+$ from NADH.

In addition to testing tissue-specific effects of NAD(P) metabolism, the application of *Lb*NOX as a tool combines two different strategies for maximizing the benefits of extending lifespan: (i) supplementation with NAD precursors (such as NR and NMN) and (ii) directly altering NADH/NAD$^+$ and NADPH/NADP$^+$ ratios (Fig. 9, A and B). By testing this strategy in *Drosophila*, we found that combining ubiquitous *Lb*NOX expression with the administration of NR in food did not result in an extended lifespan. We have tested a variety of other NAD boosting compounds and found that NR and NMN were among the most effective. In line with this, Rimal *et al.* (*61*) found that in old flies experiencing NADH-reductive stress (an elevated NADH/NAD$^+$ ratio) genetic or pharmacological inhibition of reverse electron transfer at mitochondrial CI partially normalized NADH/NAD$^+$ ratio and extended *Drosophila* lifespan. Testing different strategies will help identify the most effective combination for potential human translation to forestall aging.

Rebalancing of reducing equivalents between NAD and NADP pools

The NAD and NADP pools are interconnected via mitochondrial transhydrogenase (nicotinamide nucleotide transhydrogenase) and

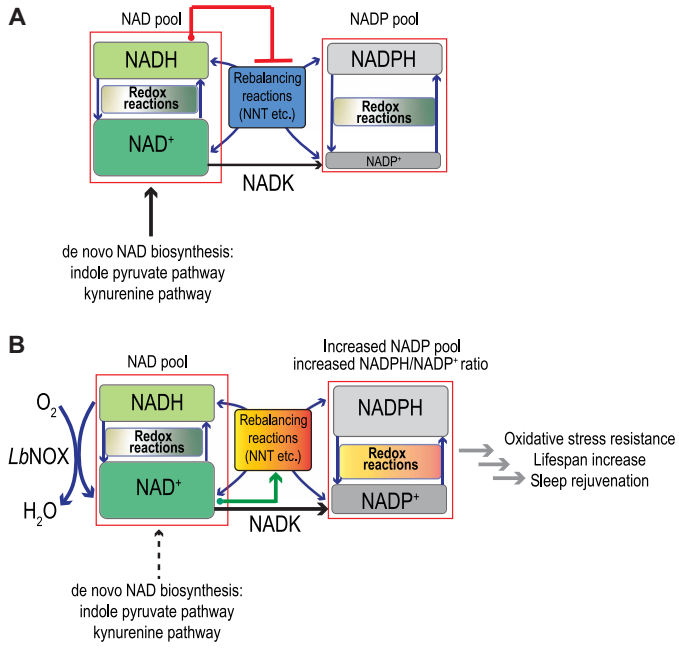

Fig. 9. Proposed model of *Lb*NOX-mediated modulation of NAD(P)(H) levels and cellular metabolism. (**A**) Under normal physiological conditions, accumulated NADH partially inhibits cellular systems responsible for NADPH regeneration (red line). (**B**) Expression of *Lb*NOX drives robust NADH consumption, resulting in increased NADPH levels and expansion of the NADP pool (green line). This shift in redox balance leads to downstream effects including enhanced stress resistance, lifespan extension, and sleep rejuvenation. Notably, *Lb*NOX expression in flies also reduces levels of metabolites associated with the indole pyruvate and kynurenine pathways. Blue arrows indicate electron flow between reduced and oxidized forms of NAD(P) and across their respective pools, which are highlighted in red boxes. Black arrows represent nonredox reactions. For clarity, NAD and NADP pools are not drawn to scale, and subcellular compartmentalization is not depicted.

multiple dehydrogenases in different cellular compartments with dual NAD(P) specificity (*54*, *62*, *63*). In our study, we also found that expression of the NADH-consuming enzyme (i.e., *Lb*NOX) affects both NAD(H) and NADP(H) metabolites. We observed that *Lb*NOX expression can increase NADP(H) levels and NADPH/NADP$^+$ ratio (Fig. 9, A and B). Our findings are in agreement with recent studies that identify NADPH regeneration as an important metabolic parameter under ETC inhibition and elevated NADH/NAD$^+$ (*18*, *64*, *65*). Therefore, in principle, a prooxidative shift (a decrease) in NADH/NAD$^+$ ratio promoted by *Lb*NOX can boost NADPH levels. Notably, in our measurements of NAD(P)(H) metabolites, we use enzymatic cycling and whole-body fly homogenates. Further studies are needed to better understand the role of compartment-specific changes in both NADH/NAD$^+$ and NADPH/NADP$^+$ using genetically encoded sensors in healthy aging as well as under various stress conditions. In flies (as well as in humans), the only route to produce NADP$^+$ from NAD$^+$ is NADK (both cytosolic and mitochondrial versions exist), but, unexpectedly, very little attention has been given to NADK regulation in the context of aging (*66*). One promising future direction will be to use knockout flies in concert with genetically encoded tools *Lb*NOX, TPNOX, or *Ec*STH to dissociate NAD metabolism from NADP metabolism as well as to uncouple the regulation of NADP(H) production from cellular metabolism linked to ROS.

Sleep

Sleep disturbances are observed with aging and may serve as a risk factor for developing cognitive impairment and Alzheimer's disease (*67*–*69*). *Drosophila* is a powerful genetic model system for studying sleep (*70*). Previous studies have established the importance of NAD(P) metabolism in the regulation of sleep in *Drosophila* (*39*, *40*), mice (*41*, *42*), and humans (*43*, *44*). Using *Lb*NOX allows us to test the involvement of NAD(P) metabolism in different tissues in the regulation of sleep. Excitingly, we find that perturbing NAD(P) metabolism in nonneuronal cells is sufficient to rejuvenate sleep profiles to a youthful stage. Lane *et al.* (*71*) found genetic loci for self-reported insomnia symptoms encompassing genes expressed in skeletal muscle. Using *Lb*NOX or other xenotopic tools will allow us to dissect nonneuronal mechanisms of sleep regulation.

Sex-specific effects

The regulation of aging-related processes is often sex specific, and targeting of a multitude of metabolic pathways often delays aging in one sex but not in another (*1*). In agreement with this, we observed marked sex-dependent effects of *Lb*NOX expression in *Drosophila*. These sex-specific effects of alterations in NAD metabolites are also observed in healthy humans as women have lower plasma NADH/NAD^+ ratios than men (*72*). Accordingly, Van der Velpen *et al.* (*73*) demonstrated sex-specific alterations in the levels of intermediates in NAD metabolism comparing wild-type (as well as AD-relevant) mice of different sexes. We observed that male and female flies have drastically different phenotypes under *Lb*NOX expression. In general, *Lb*NOX expression has stronger protective effects against different stresses and in extending lifespan in females than in males. In *Drosophila*, sex determination is achieved in a cell-specific manner by a balance of female determinants on the X chromosome and male determinants on the autosomes. As we observe that *Lb*NOX expression just in one tissue has a significant effect on the whole organismal physiology in a sex-specific manner, in the future, we can use available *Drosophila* tools together with *Lb*NOX to alter sex only in specific tissues to determine whether it would reverse these *Lb*NOX-associated phenotypes. This would allow studying interactions between NAD metabolism and sex-specific effects on a tissue-specific level.

Overexpression of mutated human CryAB ($CryAB^{R120G}$) was previously used to model reductive stress in both mice and flies (*22*, *74*). It is believed that $CryAB^{R120G}$ overexpression leads to protein aggregation, which triggers NRF2 activation and up-regulation of antioxidant machinery, ultimately leading to an elevated GSH/oxidized glutathione (GSSG) ratio (*13*). Xie *et al.* (*22*) demonstrated that $CryAB^{R120G}$ expression in *Drosophila* mounts impaired cardiac function when expressed in the heart or severely impaired eye development when expressed in the eye. The authors concluded that $CryAB^{R120G}$ expression in *Drosophila* leads to reductive stress, at least in part through an elevated GSH/GSSG ratio by demonstrating that RNA interference–mediated knockdowns of multiple NADPH-producing enzymes (G6PD, PGD, IDH, and MEN) suppress this $CryAB^{R120G}$ pathology (*22*). Paradoxically, our study shows that the eye phenotype is only rescued by *Lb*NOX expression line 128, in which *Lb*NOX expression leads to an increase in NADPH levels and NADPH/$NADP^+$ ratio (Figs. 2E and 1E). We also note that the major difference between males and females expressing *Lb*NOX is that in males, we observe a clear decrease in the total NADH/NAD^+ ratio, while in females, this is not the case (Fig. 1, B and C). Reductive stress is a relatively unexplored concept, and the exact mechanism by which reductive stress contributes to impaired cardiac function or eye pathology is unknown (*22*). Nonetheless, our results suggest a useful paradigm to study this phenomenon in more depth.

Limitations

(i) Although we observed tissue-specific effects of *Lb*NOX expression, we do not know whether these effects are attributed to NAD(P)(H) changes, specifically in these tissues, indirectly through systemic NAD(P)(H) changes, through secondary effects associated with perturbed downstream redox signaling, or through other NAD(P)(H)-independent effects associated with *Lb*NOX expression. (ii) As the known muscle-specific GS lines are leaky or have nonspecific effects on the expression of nuclear-encoded mitochondrial genes (*37*, *38*), which could potentially complicate the interpretation of muscle-specific *Lb*NOX expression using the muscle-specific GS system, we could not use muscle-specific GS lines to validate our findings with the GAL80ts system. (iii) In this study, we were only able to examine *Drosophila* expressing the nontargeted version of *Lb*NOX, which is assumed to be predominantly cytoplasmic but may also be transported to various subcellular compartments or indirectly affect NAD(P)(H) levels in other compartments. Future work should characterize compartment-specific versions of *Lb*NOX and compare their effects in parallel with the current non-targeted version. (iv) Most of the experiments use the GAL4/GAL80ts system because of its advantages: stronger expression than the GS system, nonleakiness, lack of mosaic expression patterns in the target tissue, ubiquitous expression, and nonchemical transgene induction. However, the main limitations of this system are the use of a nonoptimal temperature to induce transgene expression and the possibility of observing substantial changes due to differences in genetic background rather than transgene expression.

MATERIALS AND METHODS

Generation of *Lb*NOX flies

*Lb*NOX was amplified from the pUC57-*Lb*NOX plasmid obtained from Addgene (#75285) and cloned into the pWALIUM10-roe vector according to the standard protocol (both the plasmid sequence and the reported protocol are available at https://fgr.hms.harvard.edu/trip-plasmid-vector-sets). Transgenic flies carrying the *Lb*NOX transgene on either the 2nd (line #128) or the 3rd (line #129) chromosome were generated following the standard protocol at the DRSC/TRiP Functional Genomics Resources Center (https://fgr.hms.harvard.edu/protocols).

Drosophila stocks and maintenance

Flies (*Drosophila melanogaster*) were maintained on a standard cornmeal medium, commercially obtained as "Fly Food J" from LabExpress (Ann Arbor, MI) containing yeast, dextrose, sucrose, and molasses and reared at 25°C in incubators with a 12-hour light-dark cycle. For all experiments, the closest genetic control flies (used to generate the transgenic line) were used and treated the same way as the experimental flies. The list of fly stocks used in the study is detailed in the Key Resource Table (table S3). Flies with GS driver were reared at 25°C throughout the experiment. Flies with $Gal80^{ts}$ driver were reared at 18°C during development and were moved to 29°C post collection.

Acquisition of eye pictures and rough eye phenotype (REP) quantification

All the flies were collected within 24 hours of eclosion and were aged for 5 days at 25°C followed by snap-freezing on dry ice. For each genotype, five to six individual fly eyes were imaged using Nikon SMZ1270 microscope at different focal lengths and were combined later using the freely available CombineZP software. For REP quantification, six to nine flies were scored per genotype. Quantification was done by scoring eye images for the presence or absence of four features: (i) loss of pigmentation, (ii) extra interommatidial bristles, (iii) disrupted eye curvature or shape, and (iv) fused ommatidia. Presence was scored as 1, absence as 0, and a relatively enhanced or suppressed feature as ±0.5.

Lifespan analysis

Flies were collected within 24 to 48 hours from eclosion and allowed to mate for 1 to 2 days followed by sorting by sex under CO_2 anesthesia. Postseparation, the flies were reared at standard density (20 to 25 flies per vial) at 25°C (unless otherwise mentioned) and 60% humidity with 12 hours on/off light cycle. The flies were flipped onto fresh vials every 2 days, and the dead flies were counted. For flies carrying GS element (GS lines), gene expression was induced by feeding flies on fly food containing the chemical RU-486 (Cayman chemicals, item no. 10006317) dissolved in ethanol at a final concentration of 200 μM (86 μg/ml). The control flies were reared on food containing equal amounts of the vehicle/solvent (ethanol).

Starvation assay

All the flies were allowed to mate for 1 to 2 days posteclosion followed by separation by sex and were reared at appropriate temperature for one week or 3 weeks as referred in the text. For induction of starvation stress, the separated flies were placed on vials having freshly prepared 1% agar. The total fly density per vial was kept between 12 and 15 flies, and the number of dead flies was counted twice a day (morning and evening) until all flies died.

Oxidative stress assay

All the flies were allowed to mate for 1 to 2 days posteclosion followed by separation by sex and were reared at appropriate temperature for 1 week or 3 weeks as referred in the text. For induction of oxidative stress, the flies were placed on freshly prepared food containing 1% agar, 5% sucrose, and 10 mM of paraquat. The total fly density per vial was kept between 12 and 15 flies, and the number of dead flies was counted twice a day (morning and evening) until all died.

Climbing assay

Flies were collected, mated, and maintained in the same way as described for the lifespan analysis. For each genotype, 110 to 120 flies were typically scored (10 independent replicate vials were used, each containing 11 to 12 flies). To assess climbing ability, the flies were transferred into an empty vial (90 mm in height, marked at the midpoint), which was tapped sharply on the table three times to initiate a negative geotaxis response, followed by counting the number of flies that crossed the midline after 10 s. Three trials were conducted for each vial. After testing, the flies were returned to a regular fly food vial. The same set of flies was tested every week until 5 weeks of age. During aging, vials containing fewer than five flies were not tested.

Quantification of NAD^+, NADH, $NADP^+$, and NADPH

Ten flies were placed into Precellys Hard Tissue Homogenizing Kit 2-ml Reinforced Tubes (Precellys, # P000916-LYSK0-A.0), and, immediately, 600 μl of wet ice-cold 1:1 mixture of phosphate-buffered saline (PBS) and 1% dodecyl trimethylammonium bromide (DTAB) in 0.2 M NaOH was added. Flies were homogenized using Bertin Precellys 24 Lysis Biological Tissue Homogenizer. Immediately after homogenization step tubes were centrifuged at 21,000 rcf speed for 10 min to pellet down debris, and two 200 μl aliquots were used to process oxidized and reduced nucleotides as previously described (*54*) with minor modifications indicated below. When transferred to all-white 96-well plates, the samples for NADH and NAD^+ determination were diluted five times with the dilution buffer (equal volumes of PBS, base solution with 1% DTAB, 0.4N HCl, and 0.5M Trizma) containing 10 μM ascorbic acid (10 μl sample + 40 μl of the dilution buffer). This dilution is critical to maintain NAD(H) nucleotides in the linear range of the calibration curve. Samples for NADPH and $NADP^+$ estimation were not diluted as flies contain ~10 times smaller NADP pool compared to NAD pool. Calibration curves were constructed for NAD^+, NADH, $NADP^+$, and NADPH nucleotides prepared in the dilution buffer containing 10 μM ascorbic acid. To each 50 μl of samples and standards in all-white 96-well plates, another 50 μl of the corresponding NAD/NADH-Glo or NADP/NADPH-Glo Detection Reagent (Promega, catalog no. G9071 and G9081) were added, and luminescence was measured over 2 hours using BioTek Cytation C10 Confocal Imaging Reader (Agilent Technologies). In our luminescence-based assays, we do not take end-time points. Instead, we monitor changes in luminescence over time and take a derivative of that change in the linear portion of the reaction progress curve to maximize the accuracy and reproducibility of our measurements (both samples and standards). In all figures, we report the total amount of nucleotides in picomols from 10 flies taking into account all dilutions during sample preparation.

Immunoblotting

For immunoblot analysis, five adult flies were lysed in radioimmunoprecipitation assay lysis buffer (Cell Signaling Technology) with added phosphatase and protease inhibitors (Roche), using the bullet blender tissue homogenizer. The lysates were resolved on mini-Protean TGX gel (Bio-Rad) by electrophoresis followed by transfer on polyvinylidene difluoride membrane (Immobilon P, Millipore), blocked in tris-buffered saline Tween-20 buffer (Cell Signaling Technology) containing 2.5% dry milk, and probed with the mentioned antibodies diluted in this buffer. For detecting *L*bNOX, anti-FLAG antibody 12C6c (DHSB) was used at 1:4000 dilution. For loading control, antibody against β-actin (13E5, Cell Signaling technology) was used at 1:1000 dilution.

Metabolomics

Metabolic profiling was performed as previously described (*75*). Briefly, 10 to 20 flies per sample (four biological replicates) were collected, and intracellular metabolites were extracted using 80% (v/v) aqueous methanol. Liquid chromatography was performed on an Xbridge BEH amide HILIC column (Waters) with a Vanquish UHPLC system (Thermo Fisher Scientific). Solvent A was 95:5 water:acetonitrile with 20 mM ammonium acetate and 20 mM ammonium hydroxide at pH 9.4. Solvent B was acetonitrile. The gradient used for metabolite separation was 0 min, 90% B; 2 min, 90% B; 3 min, 75%; 7 min, 75% B; 8 min, 70% B, 9 min, 70% B; 10 min, 50% B; 12 min, 50% B; 13 min,

25% B; 14 min, 25% B; 16 min, 0% B, 21 min, 0% B; 21 min, 90% B; and 25 min, 90% B. MS analysis was performed on an Orbitrap Exploris 480 mass spectrometer (Thermo Fisher Scientific) by electrospray ionization with parameters as follows: scan-mode, full MS; spray voltage, 3.6 kV (positive) and −3.2 kV (negative); capillary temperature, 320°C; sheath gas, 40 arb; aux gas, 7 arb; resolution, 120,000 (full MS); scan m/z range 70 to 1000. Web-based platform MetaboAnalyst was used to analyze and visualize metabolomics data.

Sleep measurements

DAM from Trikinetics Inc. (Waltham MA, USA) were used to monitor sleep and activity in flies. One- or 3-week-old flies (as mentioned in the Results section) were housed individually inside borosilicate glass tubes (65-mm length, 5-mm diameter) containing regular fly food at one end (coated with paraffin wax to avoid drying) and a cotton plug at the other end. Caution was taken while loading the 3-week-old flies to not expose them to CO_2 longer than 3 min while loading. Locomotor activity data were collected under LD (12-hour light/12-hour dark). Locomotor activity was recorded over a period of 4 days, and sleep was analyzed using ShinyR-DAM (https://karolcichewicz.shinyapps.io/shinyr-dam/). For all the sleep-related plots, the data were analyzed over 2 days (day 3 and day 4 from the start of experiment).

NAD precursor supplementation

The flies were collected within 24 to 48 hours from eclosion and allowed to mate for a day followed by sorting by sex under CO_2 anesthesia. Postseparation, the flies were placed on fly food containing specific NAD precursor. The flies were flipped onto fresh food vials every 2 days throughout the treatment. The following NAD precursors were used in the study: NA from Sigma-Aldrich, catalog no. N4126; NAC from Sigma-Aldrich, catalog no. A7250; BHB from Sigma-Aldrich, catalog no. 54965; NR chloride from Selleckchem, catalog no. S2935 was used for NAD^+ measurements; NR from Cayman Chemical, catalog no. 36941 was used for lifespan analysis; and NMN from Cayman Chemical, catalog no. 32883.

Supplementary Materials

This PDF file includes:

Figs. S1 to S6
Tables S1 to S3

REFERENCES

1. A. A. Parkhitko, E. Filine, S. E. Mohr, A. Moskalev, N. Perrimon, Targeting metabolic pathways for extension of lifespan and healthspan across multiple species. *Ageing Res. Rev.* **64**, 101188 (2020).
2. E. Katsyuba, M. Romani, D. Hofer, J. Auwerx, NAD^+ homeostasis in health and disease. *Nat. Metab.* **2**, 9–31 (2020).
3. S. Lautrup, D. A. Sinclair, M. P. Mattson, E. F. Fang, NAD^+ in brain aging and neurodegenerative disorders. *Cell Metab.* **30**, 630–655 (2019).
4. A. J. Covarrubias, R. Perrone, A. Grozio, E. Verdin, NAD^+ metabolism and its roles in cellular processes during ageing. *Nat. Rev. Mol. Cell Biol.* **22**, 119–141 (2021).
5. W. Xiao, R. S. Wang, D. E. Handy, J. Loscalzo, NAD(H) and NADP(H) redox couples and cellular energy metabolism. *Antioxid. Redox Signal.* **28**, 251–272 (2018).
6. C. C. S. Chini, J. D. Zeidler, S. Kashyap, G. Warner, E. N. Chini, Evolving concepts in NAD^+ metabolism. *Cell Metab.* **33**, 1076–1087 (2021).
7. A. Peluso, M. V. Damgaard, M. A. S. Mori, J. T. Treebak, Age-dependent decline of NAD^+-universal truth or confounded consensus? *Nutrients* **14**, 101 (2022).
8. L. Rajman, K. Chwalek, D. A. Sinclair, Therapeutic potential of NAD-boosting molecules: The in vivo evidence. *Cell Metab.* **27**, 529–547 (2018).
9. M. V. Damgaard, J. T. Treebak, What is really known about the effects of nicotinamide riboside supplementation in humans. *Sci. Adv.* **9**, eadi4862 (2023).
10. J. Zhang, H. L. Wang, S. Lautrup, H. L. Nilsen, J. T. Treebak, L. O. Watne, G. Selbaek, L. E. Wu, T. Omland, E. Pirinen, T. C. Cheung, J. Wang, M. Ziegler, O. B. Tysnes, R. Zapata-Perez, S. Bruzzone, C. Canto, M. Deleidi, G. E. Janssens, R. H. Houtkooper, M. Scheibye-Knudsen, M. Koshizaka, K. Yokote, E. Verdin, V. A. Bohr, C. Tzoulis, D. A. Sinclair, E. F. Fang, Emerging strategies, applications and challenges of targeting NAD^+ in the clinic. *Nat. Aging* **5**, 1704–1731 (2025).
11. A. A. Parkhitko, V. Cracan, Xenotopic synthetic biology: Prospective tools for delaying aging and age-related diseases. *Sci. Adv.* **11**, eadu1710 (2025).
12. D. V. Titov, V. Cracan, R. P. Goodman, J. Peng, Z. Grabarek, V. K. Mootha, Complementation of mitochondrial electron transport chain by manipulation of the NAD^+/NADH ratio. *Science* **352**, 231–235 (2016).
13. W. Xiao, J. Loscalzo, Metabolic responses to reductive stress. *Antioxid. Redox Signal.* **32**, 1330–1347 (2020).
14. E. C. Lien, N. Vu, A. M. Westermark, L. V. Danai, A. N. Lau, Y. Gultekin, M. A. Kukurugya, B. D. Bennett, M. G. Vander Heiden, Effects of aging on glucose and lipid metabolism in mice. *Aging Cell* **24**, e14462 (2025).
15. R. Yang, Z. Guo, B. Li, NADH reductive stress drives metabolic reprogramming. *Trends Cell Biol.* S0962–8924(25)00157-6 (2025).
16. S. E. McGuire, P. T. Le, A. J. Osborn, K. Matsumoto, R. L. Davis, Spatiotemporal rescue of memory dysfunction in *Drosophila*. *Science* **302**, 1765–1768 (2003).
17. R. Yang, C. Yang, L. Ma, Y. Zhao, Z. Guo, J. Niu, Q. Chu, Y. Ma, B. Li, Identification of purine biosynthesis as an NADH-sensing pathway to mediate energy stress. *Nat. Commun.* **13**, 7031 (2022).
18. E. Balsa, E. A. Perry, C. F. Bennett, M. Jedrychowski, S. P. Gygi, J. G. Doench, P. Puigserver, Defective NADPH production in mitochondrial disease complex I causes inflammation and cell death. *Nat. Commun.* **11**, 2714 (2020).
19. S. E. McGuire, Z. Mao, R. L. Davis, Spatiotemporal gene expression targeting with the TARGET and gene-switch systems in *Drosophila*. *Sci. STKE* **2004**, pl6 (2004).
20. M. Mladenov, L. Lubomirov, O. Grisk, D. Avtanski, V. Mitrokhin, I. Sazdova, M. Keremidarska-Markova, Y. Danailova, G. Nikolaev, R. Konakchieva, H. Gagov, Oxidative stress, reductive stress and antioxidants in vascular pathogenesis and aging. *Antioxidants (Basel)* **12**, 1126 (2023).
21. A. G. Manford, F. Rodriguez-Perez, K. Y. Shih, Z. Shi, C. A. Berdan, M. Choe, D. V. Titov, D. K. Nomura, M. Rape, A cellular mechanism to detect and alleviate reductive stress. *Cell* **183**, 46–61.e21 (2020).
22. H. B. Xie, A. Cammarato, N. S. Rajasekaran, H. Zhang, J. A. Suggs, H. C. Lin, S. I. Bernstein, I. J. Benjamin, K. G. Golic, The NADPH metabolic network regulates human αB-crystallin cardiomyopathy and reductive stress in *Drosophila melanogaster*. *PLOS Genet.* **9**, e1003544 (2013).
23. P. Vicart, A. Caron, P. Guicheney, Z. Li, M. C. Prevost, A. Faure, D. Chateau, F. Chapon, F. Tome, J. M. Dupret, D. Paulin, M. Fardeau, A missense mutation in the αB-crystallin chaperone gene causes a desmin-related myopathy. *Nat. Genet.* **20**, 92–95 (1998).
24. C. R. Reczek, K. Birsoy, H. Kong, I. Martinez-Reyes, T. Wang, P. Gao, D. M. Sabatini, N. S. Chandel, A CRISPR screen identifies a pathway required for paraquat-induced cell death. *Nat. Chem. Biol.* **13**, 1274–1279 (2017).
25. G. Roman, K. Endo, L. Zong, R. L. Davis, P[Switch], a system for spatial and temporal control of gene expression in *Drosophila melanogaster*. *Proc. Natl. Acad. Sci. U.S.A.* **98**, 12602–12607 (2001).
26. T. Osterwalder, K. S. Yoon, B. H. White, H. Keshishian, A conditional tissue-specific transgene expression system using inducible GAL4. *Proc. Natl. Acad. Sci. U.S.A.* **98**, 12596–12601 (2001).
27. E. F. Fang, Y. Hou, S. Lautrup, M. B. Jensen, B. Yang, T. SenGupta, D. Caponio, R. Khezri, T. G. Demarest, Y. Aman, D. Figueroa, M. Morevati, H. J. Lee, H. Kato, H. Kassahun, J. H. Lee, D. Filippelli, M. N. Okur, A. Mangerich, D. L. Croteau, Y. Maezawa, C. A. Lyssiotis, J. Tao, K. Yokote, T. E. Rusten, M. P. Mattson, H. Jasper, H. Nilsen, V. A. Bohr, NAD^+ augmentation restores mitophagy and limits accelerated aging in Werner syndrome. *Nat. Commun.* **10**, 5284 (2019).
28. K. Richardson, R. Wessells, A novel panel of *Drosophila* TAFAZZIN mutants in distinct genetic backgrounds as a resource for therapeutic testing. *PLOS ONE* **18**, e0286380 (2023).
29. N. C. Yang, Y. H. Cho, I. Lee, The lifespan extension ability of nicotinic acid depends on whether the intracellular NAD^+ level is lower than the sirtuin-saturating concentrations. *Int. J. Mol. Sci.* **21**, 142 (2020).
30. V. Balan, G. S. Miller, L. Kaplun, K. Balan, Z. Z. Chong, F. Li, A. Kaplun, M. F. VanBerkum, R. Arking, D. C. Freeman, K. Maiese, G. Tzivion, Life span extension and neuronal cell protection by *Drosophila nicotinamidase*. *J. Biol. Chem.* **283**, 27810–27819 (2008).
31. F. Cavaleri, E. Bashar, Potential synergies of β-hydroxybutyrate and butyrate on the modulation of metabolism, inflammation, cognition, and general health. *J. Nutr. Metab.* **2018**, 1–13 (2018).
32. A. Fiore, P. J. Murray, Tryptophan and indole metabolism in immune regulation. *Curr. Opin. Immunol.* **70**, 7–14 (2021).

33. C. Xue, G. Li, Q. Zheng, X. Gu, Q. Shi, Y. Su, Q. Chu, X. Yuan, Z. Bao, J. Lu, L. Li, Tryptophan metabolism in health and disease. *Cell Metab.* **35**, 1304–1326 (2023).
34. M. De Giovanni, H. Chen, X. Li, J. G. Cyster, GPR35 and mediators from platelets and mast cells in neutrophil migration and inflammation. *Immunol. Rev.* **317**, 187–202 (2023).
35. M. Kaihara, J. M. Price, The metabolism of quinaldic acid, kynurenic acid, and xanthurenic acid in the rabbit. *J. Biol. Chem.* **237**, 1727–1729 (1962).
36. R. Castro-Portuguez, G. L. Sutphin, Kynurenine pathway, NAD^+ synthesis, and mitochondrial function: Targeting tryptophan metabolism to promote longevity and healthspan. *Exp. Gerontol.* **132**, 110841 (2020).
37. L. Poirier, A. Shane, J. Zheng, L. Seroude, Characterization of the *Drosophila* gene-switch system in aging studies: A cautionary tale. *Aging Cell* **7**, 758–770 (2008).
38. M. Robles-Murguia, L. C. Hunt, D. Finkelstein, Y. Fan, F. Demontis, Tissue-specific alteration of gene expression and function by RU486 and the GeneSwitch system. *NPJ Aging Mech. Dis.* **5**, 6 (2019).
39. V. Mariano, A. K. Kanellopoulos, G. Aiello, A. C. Lo, E. Legius, T. Achsel, C. Bagni, SREBP modulates the $NADP^+$/NADPH cycle to control night sleep in *Drosophila*. *Nat. Commun.* **14**, 763 (2023).
40. A. Kempf, S. M. Song, C. B. Talbot, G. Miesenbock, A potassium channel beta-subunit couples mitochondrial electron transport to sleep. *Nature* **568**, 230–234 (2019).
41. P. N. Bushana, M. A. Schmidt, M. J. Rempe, B. A. Sorg, J. P. Wisor, Chronic dietary supplementation with nicotinamide riboside reduces sleep need in the laboratory mouse. *Sleep Adv.* **4**, zpad044 (2023).
42. K. M. Ramsey, J. Yoshino, C. S. Brace, D. Abrassart, Y. Kobayashi, B. Marcheva, H. K. Hong, J. L. Chong, E. D. Buhr, C. Lee, J. S. Takahashi, S. Imai, J. Bass, Circadian clock feedback cycle through NAMPT-mediated NAD^+ biosynthesis. *Science* **324**, 651–654 (2009).
43. M. Morifuji, S. Higashi, S. Ebihara, M. Nagata, Ingestion of β-nicotinamide mononucleotide increased blood NAD levels, maintained walking speed, and improved sleep quality in older adults in a double-blind randomized, placebo-controlled study. *Geroscience* **46**, 4671–4688 (2024).
44. B. Cuenoud, Z. Huang, M. Hartweg, M. Widmaier, S. Lim, D. Wenz, L. Xin, Effect of circadian rhythm on NAD and other metabolites in human brain. *Front. Physiol.* **14**, 1285776 (2023).
45. T. S. Andreani, T. Q. Itoh, E. Yildirim, D. S. Hwangbo, R. Allada, Genetics of circadian rhythms. *Sleep Med. Clin.* **10**, 413–421 (2015).
46. C. L. Partch, C. B. Green, J. S. Takahashi, Molecular architecture of the mammalian circadian clock. *Trends Cell Biol.* **24**, 90–99 (2014).
47. A. Crocker, A. Sehgal, Genetic analysis of sleep. *Genes Dev.* **24**, 1220–1235 (2010).
48. E. J. Beckwith, A. S. French, Sleep in *Drosophila* and its context. *Front. Physiol.* **10**, 1167 (2019).
49. A. Sanz, M. Soikkeli, M. Portero-Otin, A. Wilson, E. Kemppainen, G. McIlroy, S. Ellila, K. K. Kemppainen, T. Tuomela, M. Lakanmaa, E. Kiviranta, R. Stefanatos, E. Dufour, B. Hutz, A. Naudi, M. Jove, A. Zeb, S. Vartiainen, A. Matsuno-Yagi, T. Yagi, P. Rustin, R. Pamplona, H. T. Jacobs, Expression of the yeast NADH dehydrogenase Ndi1 in *Drosophila* confers increased lifespan independently of dietary restriction. *Proc. Natl. Acad. Sci. U.S.A.* **107**, 9105–9110 (2010).
50. S. Bahadorani, J. Cho, T. Lo, H. Contreras, H. O. Lawal, D. E. Krantz, T. J. Bradley, D. W. Walker, Neuronal expression of a single-subunit yeast NADH-ubiquinone oxidoreductase (Ndi1) extends *Drosophila* lifespan. *Aging Cell* **9**, 191–202 (2010).
51. K. K. Kemppainen, J. Rinne, A. Sriram, M. Lakanmaa, A. Zeb, T. Tuomela, A. Popplestone, S. Singh, A. Sanz, P. Rustin, H. T. Jacobs, Expression of alternative oxidase in *Drosophila* ameliorates diverse phenotypes due to cytochrome oxidase deficiency. *Hum. Mol. Genet.* **23**, 2078–2093 (2014).
52. D. J. Fernandez-Ayala, A. Sanz, S. Vartiainen, K. K. Kemppainen, M. Babusiak, E. Mustalahti, R. Costa, T. Tuomela, M. Zeviani, J. Chung, K. M. O'Dell, P. Rustin, H. T. Jacobs, Expression of the *Ciona intestinalis* alternative oxidase (AOX) in *Drosophila* complements defects in mitochondrial oxidative phosphorylation. *Cell Metab.* **9**, 449–460 (2009).
53. A. A. Parkhitko, L. Wang, E. Filine, P. Jouandin, D. Leshchiner, R. Binari, J. M. Asara, J. D. Rabinowitz, N. Perrimon, A genetic model of methionine restriction extends *Drosophila* health- and lifespan. *Proc. Natl. Acad. Sci. U.S.A.* **118**, e2110387118 (2021).
54. V. Cracan, D. V. Titov, H. Shen, Z. Grabarek, V. K. Mootha, A genetically encoded tool for manipulation of $NADP^+$/NADPH in living cells. *Nat. Chem. Biol.* **13**, 1088–1095 (2017).
55. X. Pan, M. L. Heacock, E. N. Abdulaziz, S. Violante, A. L. Zuckerman, N. Shrestha, C. Yao, R. P. Goodman, J. R. Cross, V. Cracan, A genetically encoded tool to increase cellular NADH/NAD^+ ratio in living cells. *Nat. Chem. Biol.* **20**, 594–604 (2024).
56. A. A. Parkhitko, A. Singh, S. Hsieh, Y. Hu, R. Binari, C. J. Lord, S. Hannenhalli, C. J. Ryan, N. Perrimon, Cross-species identification of PIP5K1-, splicing- and ubiquitin-related pathways as potential targets for RB1-deficient cells. *PLOS Genet.* **17**, e1009354 (2021).
57. S. Yadav, A. Graham, F. Al Hammood, C. Garbark, D. Vasudevan, U. Pandey, J. M. Asara, D. Rajasundaram, A. A. Parkhitko, Unique tau- and synuclein-dependent metabolic reprogramming in neurons distinct from normal aging. *Aging Cell* **23**, e14277 (2024).
58. A. A. Parkhitko, E. Filine, M. Tatar, Combinatorial interventions in aging. *Nat. Aging* **3**, 1187–1200 (2023).
59. A. H. Brand, N. Perrimon, Targeted gene expression as a means of altering cell fates and generating dominant phenotypes. *Development* **118**, 401–415 (1993).
60. M. R. McReynolds, K. Chellappa, E. Chiles, C. Jankowski, Y. Shen, L. Chen, H. C. Descamps, S. Mukherjee, Y. R. Bhat, S. R. Lingala, Q. Chu, P. Botolin, F. Hayat, T. Doke, K. Susztak, C. A. Thaiss, W. Lu, M. E. Migaud, X. Su, J. D. Rabinowitz, J. A. Baur, NAD^+ flux is maintained in aged mice despite lower tissue concentrations. *Cell Syst.* **12**, 1160–1172.e4 (2021).
61. S. Rimal, I. Tantray, Y. Li, T. Pal Khaket, Y. Li, S. Bhurtel, W. Li, C. Zeng, B. Lu, Reverse electron transfer is activated during aging and contributes to aging and age-related disease. *EMBO Rep.* **24**, e55548 (2023).
62. R. P. Goodman, S. E. Calvo, V. K. Mootha, Spatiotemporal compartmentalization of hepatic NADH and NADPH metabolism. *J. Biol. Chem.* **293**, 7508–7516 (2018).
63. H. Y. Ho, Y. T. Lin, G. Lin, P. R. Wu, M. L. Cheng, Nicotinamide nucleotide transhydrogenase (NNT) deficiency dysregulates mitochondrial retrograde signaling and impedes proliferation. *Redox Biol.* **12**, 916–928 (2017).
64. L. Del Prado, M. Jaraiz-Rodriguez, M. Agro, M. Zamora-Dorta, N. Azpiazu, M. Calleja, M. Lopez-Manzaneda, J. de Juan-Sanz, A. Fernandez-Rodrigo, J. A. Esteban, M. Girona, A. Quintana, E. Balsa, Compensatory activity of the PC-ME1 metabolic axis underlies differential sensitivity to mitochondrial complex I inhibition. *Nat. Commun.* **15**, 8682 (2024).
65. S. Igelmann, F. Lessard, O. Uchenunu, J. Bouchard, A. Fernandez-Ruiz, M. C. Rowell, S. Lopes-Paciencia, D. Papadopoli, A. Fouillen, K. J. Ponce, G. Huot, L. Mignacca, M. Benfdil, P. Kalegari, H. M. Wahba, J. Pencik, N. Vuong, J. Quenneville, J. Guillon, V. Bourdeau, L. Hulea, E. Gagnon, L. Kenner, R. Moriggl, A. Nanci, M. N. Pollak, J. G. Omichinski, I. Topisirovic, G. Ferbeyre, A hydride transfer complex reprograms NAD metabolism and bypasses senescence. *Mol. Cell* **81**, 3848–3865.e19 (2021).
66. P. C. Bradshaw, Cytoplasmic and mitochondrial NADPH-coupled redox systems in the regulation of aging. *Nutrients* **11**, 504 (2019).
67. O. M. Bubu, M. Brannick, J. Mortimer, O. Umasabor-Bubu, Y. V. Sebastiao, Y. Wen, S. Schwartz, A. R. Borenstein, Y. Wu, D. Morgan, W. M. Anderson, Sleep, cognitive impairment, and Alzheimer's disease: A systematic review and meta-analysis. *Sleep* **40**, zsw032 (2017).
68. A. Iranzo, Sleep in neurodegenerative diseases. *Sleep Med. Clin.* **11**, 1–18 (2016).
69. J. E. Carroll, A. A. Prather, Sleep and biological aging: A short review. *Curr. Opin. Endocr. Metab. Res.* **18**, 159–164 (2021).
70. S. Dissel, Drosophila as a model to study the relationship between sleep, plasticity, and memory. *Front. Physiol.* **11**, 533 (2020).
71. J. M. Lane, S. E. Jones, H. S. Dashti, A. R. Wood, K. G. Aragam, V. T. van Hees, L. B. Strand, B. S. Winsvold, H. Wang, J. Bowden, Y. Song, K. Patel, S. G. Anderson, R. N. Beaumont, D. A. Bechtold, B. E. Cade, M. Haas, S. Kathiresan, M. A. Little, A. I. Luik, A. S. Loudon, S. Purcell, R. C. Richmond, F. Scheer, B. Schormair, J. Tyrrell, J. W. Winkelman, J. Winkelmann, H. A. I. Sleep, K. Hveem, C. Zhao, J. B. Nielsen, C. J. Willer, S. Redline, K. Spiegelhalder, S. D. Kyle, D. W. Ray, J. A. Zwart, B. Brumpton, T. M. Frayling, D. A. Lawlor, M. K. Rutter, M. N. Weedon, R. Saxena, Biological and clinical insights from genetics of insomnia symptoms. *Nat. Genet.* **51**, 387–393 (2019).
72. L. Schwarzmann, R. U. Pliquett, A. Simm, B. Bartling, Sex-related differences in human plasma NAD^+/NADH levels depend on age. *Biosci. Rep.* **41**, BSR20200340 (2021).
73. V. van der Velpen, N. Rosenberg, V. Maillard, T. Teav, J. Y. Chatton, H. Gallart-Ayala, J. Ivanisevic, Sex-specific alterations in NAD^+ metabolism in 3xTg Alzheimer's disease mouse brain assessed by quantitative targeted LC-MS. *J. Neurochem.* **159**, 378–388 (2021).
74. N. S. Rajasekaran, P. Connell, E. S. Christians, L. J. Yan, R. P. Taylor, A. Orosz, X. Q. Zhang, T. J. Stevenson, R. M. Peshock, J. A. Leopold, W. H. Barry, J. Loscalzo, S. J. Odelberg, I. J. Benjamin, Human αB-crystallin mutation causes oxido-reductive stress and protein aggregation cardiomyopathy in mice. *Cell* **130**, 427–439 (2007).
75. A. A. Parkhitko, D. Ramesh, L. Wang, D. Leshchiner, E. Filine, R. Binari, A. L. Olsen, J. M. Asara, V. Cracan, J. D. Rabinowitz, A. Brockmann, N. Perrimon, Downregulation of the tyrosine degradation pathway extends *Drosophila* lifespan. *eLife* **9**, e58053 (2020).

Acknowledgments: We thank K. G. Golic for providing GMR-Gal4 UAS-$CryAB^{R120G}$ stock. **Funding:** This work was supported by NIGMS R35 GM146869 (A.A.P.), NIA R01 AG082801 (A.A.P.), NIA R01 AG082696 (A.A.P.), NIA R03 AG075651 (A.A.P.), R03 CA286521 (A.A.P.), NIA P30 AG024827 pilot grant (A.A.P.), Richard King Mellon Foundation award (A.A.P.), NAM Healthy Longevity Catalyst Award (A.A.P.), NIA R03AG067301 (V.C.), NIA R21AG085012 (V.C.), NIGMS R35GM142495 (V.C), and Longevity Impetus Grants (V.C.). This is manuscript number 1078 from The Scintillon Institute. **Author contributions:** Conceptualization: A.A.P. and V.C. Methodology: S.Y., X.P., P.L.M., N.H., K.C., J.M., S.M., A.L.Z., A.K., and L.W. Investigation: A.A.P., V.C., M.K.K., S.L., A.L.Z., S.Y., and X.P. Visualization: A.A.P., V.C., S.Y., X.P., L.W., and A.L.Z. Supervision: A.A.P., V.C., and M.K.K. Writing—original draft: A.A.P., V.C., S.Y., and X.P. Writing—review and editing: A.A.P., V.C., S.Y., and X.P. **Competing interests:** V.C. is listed as an inventor on a patent

application on the therapeutic uses of *Lb*NOX and TPNOX (US patent application US20190017034A1). All other authors declare that they have no competing interests. **Data and materials availability:** All data and code needed to evaluate and reproduce the results in the paper are present in the paper and/or the Supplementary Materials.

Submitted 8 April 2025
Accepted 2 December 2025
Published 2 January 2026
10.1126/sciadv.ady0628

ScienceAdvances

Perturbation of NAD(P)H metabolism with the *Lb*NOX xenotopic tool extends lifespan and mitigates age-related changes

Shweta Yadav, Xingxiu Pan, Shengxi Li, Paige LaRae Martin, Ngoc Hoang, Kejin Chen, Aditi Karhadkar, Jatin Malhotra, Austin L. Zuckerman, Subrata Munan, Markus K. Klose, Lin Wang, Valentin Cracan, and Andrey A. Parkhitko

Sci. Adv. **12** (1), eady0628. DOI: 10.1126/sciadv.ady0628